



저작자표시-비영리-변경금지 2.0 대한민국

이용자는 아래의 조건을 따르는 경우에 한하여 자유롭게

- 이 저작물을 복제, 배포, 전송, 전시, 공연 및 방송할 수 있습니다.

다음과 같은 조건을 따라야 합니다:



저작자표시. 귀하는 원저작자를 표시하여야 합니다.



비영리. 귀하는 이 저작물을 영리 목적으로 이용할 수 없습니다.



변경금지. 귀하는 이 저작물을 개작, 변형 또는 가공할 수 없습니다.

- 귀하는, 이 저작물의 재이용이나 배포의 경우, 이 저작물에 적용된 이용허락조건을 명확하게 나타내어야 합니다.
- 저작권자로부터 별도의 허가를 받으면 이러한 조건들은 적용되지 않습니다.

저작권법에 따른 이용자의 권리는 위의 내용에 의하여 영향을 받지 않습니다.

이것은 [이용허락규약\(Legal Code\)](#)을 이해하기 쉽게 요약한 것입니다.

[Disclaimer](#)

Doctoral Thesis of Philosophy

**Hepatoprotective effects of norgalanthamine on
carbon tetrachloride (CCl₄)-induced liver injury
in mice**

Department of Veterinary Medicine

GRADUATE SCHOOL

JEJU NATIONAL UNIVERSITY

Nayeon Yang

2021. 2.

Hepatoprotective effects of norgalanthamine on carbon tetrachloride (CCl₄)-induced liver injury in mice


Nayeon Yang

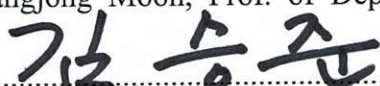
(Supervised by Professor Taekyun Shin)


A thesis submitted in partial fulfillment of the requirement for the degree of Doctor
of Veterinary Medicine

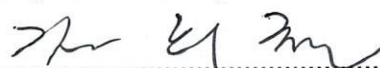
2020. 12.

This thesis has been examined and approved.


.....
Thesis director, Changjong Moon, Prof. of Dept. of Veterinary Medicine


.....
Seungjoon Kim, Prof. of Dept. of Veterinary Medicine


.....
Meejung Ahn, Prof. of Dept. of Animal Science


.....
Heechul Kim, Dr. of Research Promotion Team, KAIST


.....
Taekyun Shin, Prof. of Dept. of Veterinary Medicine

2020.12.15

Department of Veterinary Medicine

GRADUATE SCHOOL

JEJU NATIONAL UNIVERSITY

CONTENTS

List of Abbreviation	-----	1
List of Figures	-----	2
List of Tables	-----	4
General Introduction	-----	5
References	-----	16

1 Abstract	-----	27
2 Introduction	-----	29
3 Materials and methods	-----	31
4 Results	-----	42
5 Discussion	-----	63
References	-----	68
Abstract in Korean	-----	77
Acknowledgements	-----	79

List of Abbreviations

ALT	Alanine aminotransferase
ap2	Adipocyte protein-2
α -SMA	Alpha smooth muscle actin
AST	Aspartate aminotransferase
CAT	Catalase
CCl ₄	Carbon tetrachloride
DPCs	Dermal papilla cells
HO-1	Heme oxygenase-1
Iba-1	Ionized calcium-binding protein-1
MCP-1	monocyte chemoattractant protein-1
NG	Norgalanthamide
Nrf-2	Nuclear factor erythroid 2-related factor 2
IL	Interleukin
PPAR γ	Peroxisome proliferator-activated receptor gamma
ROS	Reactive oxygen species
SOD	Superoxide dismutase
TNF	Tumor necrosis factor

List of Figures

Figure 1.	Three-dimensional structure of a liver lobule. -----	9
Figure 2.	Pathobiochemical sequence of events during carbon tetrachloride (CCl ₄)-induced liver damage -----	12
Figure 3.	Schematic drawing of the experimental design -----	33
Figure 4.	The effects of norgalanthamine on the serum levels of biochemical parameters in mice with CCl ₄ -induced acute liver injury -----	44
Figure 5.	Protective effects of norgalanthamine on the histology of the liver in mice with CCl ₄ -induced acute liver injury ----	47
Figure 6.	Oil red O staining of frozen sections of liver tissue from treated and untreated mice reveals lipid accumulation -----	48
Figure 7.	mRNA expression levels of CYPs in the liver -----	50
Figure 8.	Antioxidant effect of norgalanthamine in mice with CCl ₄ -induced acute liver injury -----	52
Figure 9.	Norgalanthamine pretreatment attenuates CCl ₄ -induced inflammatory responses in the liver at the transcriptional level -----	54
Figure 10.	Immunohistochemical staining of Iba-1 in liver sections --	55

Figure 11.	Real-time PCR analyses of PPAR- γ and aP2 expression in liver tissues -----	57
Figure 12.	Representative immunoblots of Nrf-2 and HO-1 and Nrf-2 and HO-1 expression relative to the β -actin level in CCl ₄ -induced acute-liver-injury mice -----	59
Figure 13.	Effects of norgalanthamine in CCl ₄ -induced chronic liver injury in mice -----	61
Figure 14.	Real-time PCR analyses of α SMA and fibronectin expression in liver tissues -----	62
Figure 15.	Schematic diagram of the proposed molecular effects of norgalanthamine in mice with CCl ₄ -induced liver injury --	66

List of Tables

Table 1. Classification of animal models of hepatotoxicity -----	10
Table 2. Most frequently studied hepatoprotective phytochemicals -----	14
Table 3. Grading score for acute liver injury -----	36
Table 4. Primary antibodies used in the present study -----	38
Table 5. Primer sequences used in the present study -----	40

General Introduction

Biological effects of *Crinum asiaticum* var. *japonicum*

Crinum asiaticum var. *japonicum* (Family: Amaryllidaceae), is an herbaceous plant of small to moderate size. The plant is distributed on South Korea's Jeju Island, and was designated Korea's 19th Natural Treasure. *Crinum asiaticum* has been used as a rheumatic remedy and as an antipyretic and antiulcer agent, and for the alleviation of local pain and fever in Korea and Malaysia (Kim *et al.*, 2006a).

Phytochemical studies on *Crinum asiaticum* var. *japonicum* have reported several phenanthridine alkaloids, triterpene alcohols, and flavonoids (Kim *et al.*, 2006b). Alkaloids isolated from the bulbs of the tribe Amaryllidaceae have shown various pharmacological effects, such as anti-inflammatory activity (Kim *et al.*, 2006a; Mahomoodally *et al.*, 2020; Samud *et al.*, 1999), antioxidant enzyme (Ghane *et al.*, 2018; Goswami *et al.*, 2020; Ilavenil *et al.*, 2011; Indradevi *et al.*, 2012; Mahomoodally *et al.*, 2020), and anti-obesity activities (Jeong *et al.*, 2016); prevention of hair loss and improvement of hair growth (Kang *et al.*, 2017; Kim *et al.*, 2010; Yoon *et al.*, 2019); cytotoxicity (Abdel-Halim *et al.*, 2004; Likhitwitayawuid *et al.*, 1993; Mahomoodally *et al.*, 2020; Min *et al.*, 2001; Weniger *et al.*, 1995); antiviral (Dominguez *et al.*, 1992; Gabrielsen *et al.*, 1992; Ieven *et al.*, 1979), antimalarial (Likhitwitayawuid *et al.*, 1993), anti-platelet (Singh *et al.*, 2011), and antineoplastic activities (Hyun *et al.*, 2008; Mahomoodally *et al.*, 2020; Pettit *et al.*, 1990); as well as effects on disease of the nervous system (Houghton *et al.*, 2004; Refaat J, 2013).

Amaryllidaceae alkaloids affect the central nervous system and have acetylcholinesterase-inhibitory, analgesic, anti-inflammatory, antiviral, antimalarial,

antitumor, or antineoplastic activity (Goswami *et al.*, 2020; He *et al.*, 2015; Hyun *et al.*, 2008; Kim *et al.*, 2006b; Refaat J, 2013) .

The major components of this plant are crinamine from the aerial parts, together with lycorine, norgalanthamine, galanthamine, and epinorgalanthamine (Endo *et al.*, 2019; Mahomoodally *et al.*, 2020; Park, 2000). Their medicinal properties were appreciated after the discovery of pancratistatin as a promising chemotherapeutic, as well as the commercialization of galanthamine for Alzheimer disease (AD) (Khumkhong *et al.*, 2019). Alkaloids isolated from the Amaryllidaceae family have a galanthamine-derived backbone and are potent acetylcholinesterase (AChE) inhibitors that have been used to treat the symptoms of AD (Lopez *et al.*, 2002; Maelicke *et al.*, 2001).

Crinamine has a potent anticancer effect in cervical cancer cells. Its cytotoxicity is selective to cervical cancer cell lines and it is more effective at inhibiting anchorage-independent tumor spheroid growth than several established chemotherapeutics. In addition, the compound activates DNA damage-independent apoptosis, reduces cell migration by downregulating key EMT inducers, and suppresses vascular endothelial growth factor-A secretion and in vivo angiogenesis (Khumkhong *et al.*, 2019). Crinamine inhibits nitric oxide production and induced inducible nitric oxide synthase (iNOS) in lipopolysaccharide (LPS)-activated macrophages (Kim *et al.*, 2006b).

Lycorine is a natural alkaloid with immense therapeutic potential. Lycorine is active at a very low concentration and has high specificity against a number of cancers both in vivo and in vitro and against various drug-resistant cancer cells (Jiang and Liu, 2018; Liu *et al.*, 2018; Roy *et al.*, 2018; Shen *et al.*, 2018; Wu *et al.*, 2018). The first reported activity of lycorine as an inhibitor of termination of

protein synthesis was found in poliovirus-infected HeLa cells (Vrijsen *et al.*, 1986). The main metabolite of lycorine degradation, ungeremine, and carbamate substitution at C-1 and C-2 of lycorine had stronger antibacterial activity toward the fish bacterial pathogen *Flavobacterium columnare* isolates than did lycorine. Lycorine shows significant inhibition of DNA topoisomerase-I activity, which is required for cell growth in parasites (Casu *et al.*, 2011; Roy *et al.*, 2018; Tan *et al.*, 2011). The lycorine precursor norbelladine acts as an anti-inflammatory compound by inhibiting NF- κ B signaling, which suppresses endplate-chondrocyte degeneration and prevents intervertebral disc degeneration (Wang *et al.*, 2018). Degradation of acetylcholine (Ach) by AChE leads to brain cholinergic dysfunction in patients with AD. Lycorine also has analgesic, choleric, and body-temperature lowering activity (Roy *et al.*, 2018).

Norgalanthamine has hair-growth promoting effects, including increasing hair-fiber length in cultured rat vibrissa follicles and increasing dermal papilla cell (DPC) proliferation (Kim *et al.*, 2010; Yoon *et al.*, 2019). Norgalanthamine can stimulate the anagen phase of the hair cycle in DPCs via activation of the ERK 1/2, PI3K/AKT, and Wnt/ β -catenin pathways (Yoon *et al.*, 2019).

These studies revealed that a component norgalanthamine possesses a variety of biological activity through cell activation signals. Little is known on the effect of norgalanthamine in oxidative stress induced in vivo models including CCl₄ induced liver injury. The biological effects of norgalanthamine remains to be further studied.

Liver is one of the most important metabolic organs

The liver is one of the most important metabolic organs of vertebrates and has

multiple functions. It receives oxygenated blood from the heart via the hepatic artery, and nutrient-rich blood from the gastrointestinal tract via the portal vein (Malarkey *et al.*, 2005). The blood flows through liver sinusoids (terminal vessels between hepatocyte cords and lined with Kupffer cells and endothelial cells), empties into the central vein, and exits the liver via the hepatic veins (Hollander *et al.*, 1987). Hepatocytes make up 70–85% of all liver cells (Baratta *et al.*, 2009). They are key functional cells with important metabolic, secretory, and endocrine functions (Treuting *et al.*, 2017). Kupffer cells, another type of liver cell, are specialized macrophages on the walls of the liver sinusoids (Baratta *et al.*, 2009). Hepatic stellate cells (HSCs) are pericytes in the space of Disse, which is located between the hepatocytes and the sinusoidal endothelium (Friedman, 2008). Quiescent HSCs can be activated in response to liver damage, leading to collagen formation, fibrosis, or cirrhosis (Friedman, 2008; Li *et al.*, 2018; Solis-Herruzo *et al.*, 2003; Zhao *et al.*, 2014). Bile is secreted by hepatocytes, and drains into biliary ductules, which are lined with epithelial cells, and leaves the liver via the bile duct (Wang *et al.*, 2017).

Animal models of hepatotoxicity

The liver filters toxic substances from the body. Hepatic damage may occur when accumulation of toxins is faster than the ability of the liver to remove them (Bigoniya P. *et al.*, 2009). Hepatotoxicity may imply chemically driven liver damage. Some medical agents when taken at very high doses but also in therapeutic ranges can injure the liver (McGill and Jaeschke, 2019). Chemicals that cause liver injury are termed hepatotoxins (Bhakuni *et al.*, 2016). Several other factors may also cause hepatotoxicity, including herbal remedies, viral infections, autoimmune disorders, intoxication, and an imbalanced diet, among others (Pandit *et al.*, 2012).

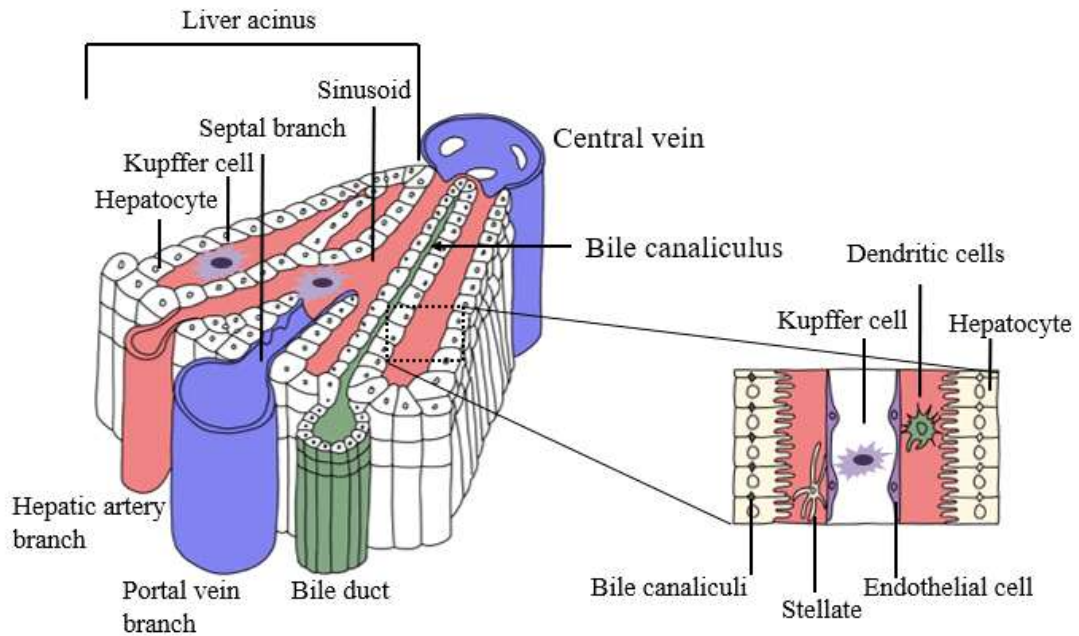


Figure 1. Three-dimensional structure of a liver lobule. Blood in the branches of the hepatic artery and portal vein enters the sinusoids, between the cords of liver cells, and courses toward the central vein, which is a tributary of the hepatic vein. Bile flows in the opposite direction, from the center out, toward the tributaries of the bile duct. Bile canaliculi are tiny channels which exist between the cell surfaces of neighboring hepatic parenchymal cells. They are supported by a delicate connective tissue stroma. Hepatic sinusoids are lined by two cell types: (1) discontinuous endothelial cells and (2) phagocytic cells of kupffer. Modified from Springer Nature Publishing AG, Adams *et al.*, Nat. Rev. Immunol., 2006.

Table 1. Classification of animal models of hepatotoxicity¹⁾

In vivo model

A Non-invasive model

- a. Chemically induced hepatotoxicity
 - CCl₄ induced
 - Thioacetamide induced
 - Dimethyl or diethyl nitrosamine induced
 - Aflatoxin induced
 - b. Drug-induced hepatotoxicity
 - NSAID induced
 - Anticancer drugs induced
 - Antibiotic induced
 - Anti-TB drugs induced
 - c. Radiation-induced hepatotoxicity
 - d. Metal-induced hepatotoxicity
 - Mercury induced
 - e. Diet-induced hepatotoxicity
 - Alcohol induced
 - High fat diet induced
-

B. Invasive model

- Bile duct ligation
 - Portal vein ligation
-

C. Genetic model

- Transgenic animal model
-

1) cited by Bhakuni et al., 2016

Mechanisms of carbon tetrachloride-induced liver injury

Carbon tetrachloride is an inorganic compound with the chemical formula CCl_4 . It is a clear liquid that evaporates easily and has a sweet odor. It is a common industrial solvent and is hepatotoxic (Abraham *et al.*, 1999). It is the most widely used hepatic toxicant in studies of liver injury involving laboratory animals (Bhakuni *et al.*, 2016). CCl_4 is metabolized in the liver by the cytochrome P450 superfamily of monooxygenases (CYP family) to the trichloromethyl radical (CCl_3^*). Subsequently, this radical reacts with nucleic acids, proteins, and lipids, thereby impairing key cellular processes and resulting in altered lipid metabolism (fatty degeneration and steatosis) and lower levels of proteins. Adduct formation between CCl_3^* and DNA triggers mutations and the formation of HCC. The formation of trichloromethylperoxy radicals (CCl_3OO^*) by oxygenation of CCl_3^* initiates lipid peroxidation and the destruction of polyunsaturated fatty acids. Consequently, the membrane permeability in all cellular compartments (mitochondria, endoplasmic reticulum, and plasma membrane) is lowered and generalized hepatic damage occurs, characterized by inflammation, fibrosis, cirrhosis, and HCC. A comprehensive summary of the pathogenic events that occur in the liver during CCl_4 -induced damage is given elsewhere. Besides its hepatotoxicity, minor acute systemic toxicity of CCl_4 has been described, particularly in the peritoneum, mucosa, respiratory tract, and central nervous system (Brattin *et al.*, 1985; Recknagel *et al.*, 1989; Scholten *et al.*, 2015; Starkel and Leclercq, 2011).

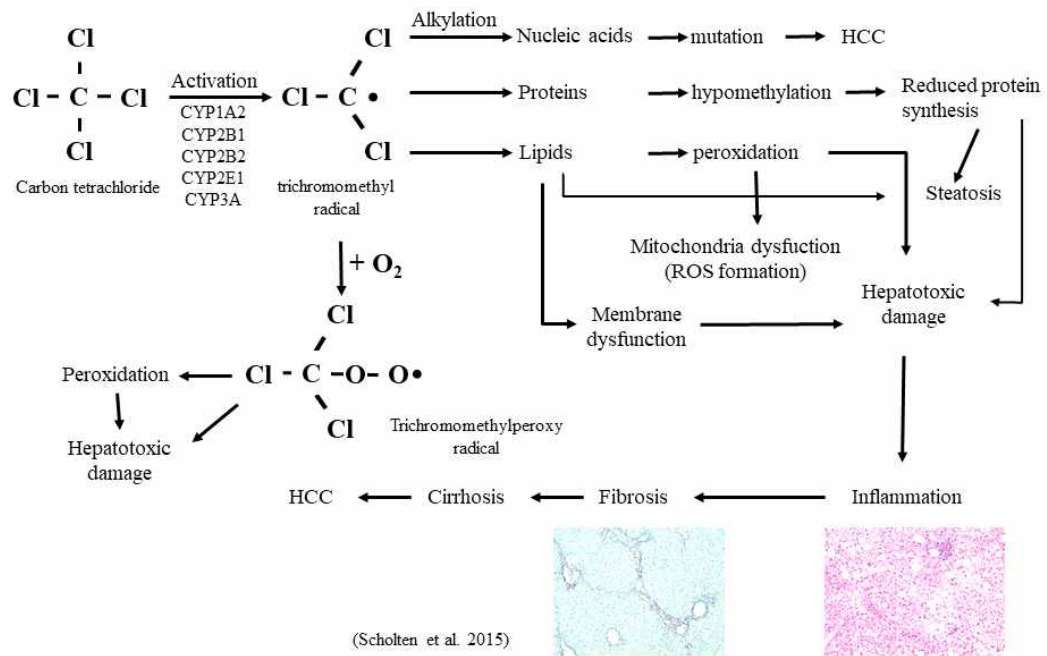


Figure 2. Pathobiochemical sequence of events during carbon tetrachloride (CCl₄)-induced liver damage. In the liver, CCl₄ is metabolized by cytochrome P450 (CYP) enzymes to a trichloromethyl radical that can be further oxygenated to the trichloromethylperoxy radical. Both radicals are highly reactive and induce complex cellular alterations that result in hepatotoxic damage, inflammation, fibrosis, cirrhosis and hepatocellular carcinoma (HCC). Modified from Scholten *et al.*, 2015.

Hepatoprotective effects of medicinal plants

There are approximately 75,000 higher-plant species, about 10% of which have been used in traditional remedies. However, perhaps only about 1% of these have been recognized through scientific studies to have therapeutic value when used in extract form. One of the most common causes of liver disease is inflammation, often resulting from abuse of alcohol, poor diet, or malnutrition. Drug-induced liver damage or liver dysfunction is an important public-health challenge. According to the United States Acute Liver Failure Study Group, drug-induced liver injury accounts for more than 50% of acute liver failure, including hepatotoxicity caused by overdose of acetaminophen (39%) and idiosyncratic liver injury triggered by other drugs. Hepatic cell injury is caused by various toxic chemicals (certain antibiotics, chemotherapeutic agents, carbon tetrachloride, and thioacetamide), excessive alcohol consumption, and microbes. It is clear that medicinal plants play an important role in a variety of diseases. Different medicinal herbs and plants extracts have potent hepatoprotective activity in animal models. Extracts of leaves and some medicinal plants have therapeutic potential for hepatic diseases (Roy *et al.*, 2014). Use of substances from natural sources for phytotherapy of various diseases, including liver diseases, is desirable because they are relatively inexpensive and widely available. Silymarin and resveratrol are two of many examples of natural substances with marked hepatoprotective potential as a result of their antioxidant, anti-inflammatory, and liver-regenerative capabilities (Farghali *et al.*, 2015; Shakya, 2020).

The CCl₄-injured liver has been used to test the efficacy of anti-inflammatory agents, with a particular focus on therapies based on a single compound.

Table 2. Most frequently studied hepatoprotective phytochemicals²⁾

Compound	Major food resources	Major biological activity
Silymarin (Silybin)	Seeds of milk thistle Silybum marianum	Antioxidant, anti-inflammatory, anti-fibrotic, protein synthesis increasing/regenerative, membrane stabilizing, and toxin blocking activities; it reduces tumor cell proliferation, angiogenesis as well as insulin resistance
Curcumin	Rhizomes turmeric (<i>Curcuma longa</i>), yellow spice	Antioxidant, anti-inflammatory, antifibrotic, anticancer, anti-aggregatory, and potent cytochrome P450 inhibitory activities
Quercetin	Fruits (apples, cranberries), vegetables (broccoli, onion), tea leaves (<i>Camellia</i> <i>sinensis</i>), grains (buckwheat)	Antioxidant, anti-inflammatory, and anticancer activities
Resveratrol	Berries, grapes, wine, peanuts	Antioxidant, anti-inflammatory, antiaging, antithrombotic, antifibrogenic, and regenerative properties; it reduces tumor cell proliferation, angiogenesis as well as insulin resistance

Glycyrrhizin	Root of Indian licorice (<i>Glycyrrhiza glabra</i>)	Antioxidant, anti-inflammatory, anticancer, antiviral, and immunomodulatory activities
Colchicine	Plants of the genus <i>Colchicum</i> (autumn crocus, <i>Colchicum</i> autumnale)	Anti-inflammatory, antifibrotic, and immunomodulatory activities

2) cited by Farghali et al., 2015; Shakya, 2020

References

- Abdel-Halim, O.B., Morikawa, T., Ando, S., Matsuda, H., Yohikawa, M., 2004. New crinine-type alkaloids with inhibitory effect on induction of inducible nitric oxide synthase from *Crinum yemense*. *J Nat Prod* 67(7), 1119-1124.
- Abraham, P., Wilfred, G., Cathrine, 1999. Oxidative damage to the lipids and proteins of the lungs, testis and kidney of rats during carbon tetrachloride intoxication. *Clin Chim Acta* 289(1-2), 177-179.
- Adams, D.H., Eksteen, B., 2006. Aberrant homing of mucosal T cells and extra-intestinal manifestations of inflammatory bowel disease. *Nat Rev Immunol* 6(3), 244-251.
- Baratta, J.L., Ngo, A., Lopez, B., Kasabwalla, N., Longmuir, K.J., Robertson, R.T., 2009. Cellular organization of normal mouse liver: a histological, quantitative immunocytochemical, and fine structural analysis. *Histochem Cell Biol* 131(6), 713-726.
- Bhakuni, G.S., Bedi, O., Bariwal, J., Deshmukh, R., Kumar, P., 2016. Animal models of hepatotoxicity. *Inflamm Res* 65(1), 13-24.
- Bigoniya, P., Singh, C.S., Shukla, A., 2009. A Comprehensive Review of Different Liver Toxicants Used in Experimental Pharmacology. *IJPSDR* 1(3), 124-135.

- Brattin, W.J., Glende Jr, E.A., Recknagel, R.O., 1985. Pathological mechanisms in carbon tetrachloride hepatotoxicity. *J Free Radic Biol Med* 1(1), 27-38.
- Casu, L., Cottiglia, F., Leonti, M., De Logu, A., Agus, E., Tse-Dinh, Y.C., Lombardo, V., Sissi, C., 2011. Ungeremine effectively targets mammalian as well as bacterial type I and type II topoisomerases. *Bioorg Med Chem Lett* 21(23), 7041-7044.
- Dominguez, X.A., B, G.E., Rombold, C., Utz, W., Achenbach, H., 1992. Neolignans, Norneolignans, and Other Components from *Krameria sonora* 1. *Planta Med* 58(4), 382-383.
- Endo, Y., Sugiura, Y., Funasaki, M., Kagechika, H., Ishibashi, M., Ohsaki, A., 2019. Two new alkaloids from *Crinum asiaticum* var. *japonicum*. *J Nat Med* 73(3), 648-652.
- Farghali, H., Canova, N.K., Zakhari, S., 2015. Hepatoprotective properties of extensively studied medicinal plant active constituents: possible common mechanisms. *Pharm Biol* 53(6), 781-791.
- Friedman, S.L., 2008. Hepatic stellate cells: protean, multifunctional, and enigmatic cells of the liver. *Physiol Rev* 88(1), 125-172.
- Gabrielsen, B., Monath, T.P., Huggins, J.W., Kefauver, D.F., Pettit, G.R., Groszek, G., Hollingshead, M., Kirsi, J.J., Shannon, W.M., Schubert, E.M., et al., 1992.

- Antiviral (RNA) activity of selected Amaryllidaceae isoquinoline constituents and synthesis of related substances. *J Nat Prod* 55(11), 1569-1581.
- Ghane, SG., Attar, UA., Yadav, PB., Lekhak, MM., 2018. Antioxidant, anti-diabetic, acetylcholinesterase inhibitory potential and estimation of alkaloids (lycorine and galanthamine) from *Crinum* species: An important source of anticancer and anti-Alzheimer drug. *Ind Crops Prod* 125, 168-177.
- Goswami, S., Das, R., Ghosh, P., Chakraborty, T., Barman, A., Ray, S., 2020. Comparative antioxidant and antimicrobial potentials of leaf successive extract fractions of poison bulb, *Crinum asiaticum* L. *Ind Crops Prod* 154, 112667.
- He, M., Qu, C., Gao, O., Hu, X., Hong, X., 2015. Biological and pharmacological activities of amaryllidaceae alkaloids. *RSC Adv* 5(21), 16562-16574.
- Hollander, C.F., van Bezooijen, C.F., Solleveld, H.A., 1987. Anatomy, function and aging in the mouse liver. *Arch Toxicol Suppl* 10, 244-250.
- Houghton, P.J., Agbedahunsi, J.M., Adegbulugbe, A., 2004. Choline esterase inhibitory properties of alkaloids from two Nigerian *Crinum* species. *Phytochemistry* 65(21), 2893-2896.
- Hyun, J.H., Kang, J.I., Kim, S.C., Kim, E., Kang, J.H., Kwon, J.M., Park, D.B., Lee, Y.J., Yoo, E.S., Kang, H.K., 2008. The Effects of *Crinum asiaticum* on the Apoptosis Induction and the Reversal of Multidrug Resistance in HL-60/MX2. *Toxicol Res* 24(1), 29-36.

- Ieven, M., Vanden Berghe, D.A., Mertens, F., Vlietinck, A., Lammens, E., 1979. Screening of higher plants for biological activities. I. Antimicrobial activity. *Planta Med* 36(4), 311-321.
- Ilavenil, S., Kaleeswaran, B., Sumitha, P., Tamilvendan, D., Ravikumar, S., 2011. Protection of human erythrocyte using *Crinum asiaticum* extract and lycorine from oxidative damage induced by 2-amidinopropane. *Saudi J Biol Sci* 18(2), 181-187.
- Indradevi, S., Ilavenil, S., Kaleeswaran, B., Srigopalram, S., Ravikumar, S., 2012. Ethanolic extract of *Crinum asiaticum* attenuates hyperglycemia-mediated oxidative stress and protects hepatocytes in alloxan induced experimental diabetic rats. *J King Saud Univ Sci* 24(2), 171-177.
- Jeong, Y.J., Sohn, E.H., Jung, Y.H., Yoon, W.J., Cho, Y.M., Kim, I., Lee, S.R., Kang, S.C., 2016. Anti-obesity effect of *Crinum asiaticum* var. *japonicum* Baker extract in high-fat diet-induced and monogenic obese mice. *Biomed Pharmacother* 82, 35-43.
- Jiang, Q.Q., Liu, W.B., 2018. Lycorine inhibits melanoma A375 cell growth and metastasis through the inactivation of the PI3K/AKT signaling pathway. *Med Sci (Paris)* 34 Focus issue F1, 33-38.
- Kang, J.I., Choi, J.H., Lee, J.G., Yoo, E.S., Kim, Y.H., Kang, H.K., 2017. The Mechanism of *Crinum asiaticum* var. *japonicum* on the Activation of Anagen. *Kor J Pharmacogn* 48(2), 148-154.

- Khumkhong, P., Piboonprai, K., Chaichompoo, W., Pimtong, W., Khongkow, M., Namdee, K., Jantimaporn, A., Japrun, D., Asawapirom, U., Suksamrarn, A., Iempridee, T., 2019. Crinamine Induces Apoptosis and Inhibits Proliferation, Migration, and Angiogenesis in Cervical Cancer SiHa Cells. *Biomolecules* 9(9), 494.
- Kim, S.C., Kang, J.I., Kim, M.K., Hyun, J.H., Boo, H.J., Park, D.B., Lee, Y.J., Yoo, E.S., Kim, Y.H., Kim, Y.H., Kang, H.K., 2010. Promotion effect of norgalanthamine, a component of *Crinum asiaticum*, on hair growth. *Eur J Dermatol* 20(1), 42-48.
- Kim, Y.H., Kim, K.S., Park, S.H., Lee, S.H., Kim, Y.J., Kim, Y.S., Kim, J.H., Kim, K.H., 2006a. Anti-inflammatory Activity of *Crinum asiaticum* Linne var. *japonicum* Extract and its Application as a Cosmeceutical Ingredient. *J Soc Cosmet Sci Korea* 32(1), 59-64.
- Kim, Y.H., Park, E.J., Park, M.H., Badarch, U., Woldemichael, G.M., Beutler, J.A., 2006b. Crinamine from *Crinum asiaticum* var. *japonicum* Inhibits Hypoxia Inducible Factor-1 Activity But Not Activity of Hypoxia Inducible Factor-2. *Biol Pharm Bull* 29(10), 2140-2142.
- Li, Y., Zhu, M., Huo, Y., Zhang, X., Liao, M., 2018. Anti-fibrosis activity of combination therapy with epigallocatechin gallate, taurine and genistein by regulating glycolysis, gluconeogenesis, and ribosomal and lysosomal signaling pathways in HSC-T6 cells. *Exp Ther Med* 16(6), 4329-4338.

- Likhitwitayawuid, K., Angerhofer, C.K., Chai, H., Pezzuto, J.M., Cordell, G.A., Ruangrunsi, N., 1993. Cytotoxic and antimalarial alkaloids from the bulbs of *Crinum amabile*. *J Nat Prod* 56(8), 1331-1338.
- Liu, W., Zhang, Q., Tang, Q., Hu, C., Huang, J., Liu, Y., Lu, Y., Wang, Q., Li, G., Zhang, R., 2018. Lycorine inhibits cell proliferation and migration by inhibiting ROCK1/cofilin-induced actin dynamics in HepG2 hepatoblastoma cells. *Oncol Rep* 40(4), 2298-2306.
- Lopez, S., Bastida, J., Viladomat, F., Codina, C., 2002. Acetylcholinesterase inhibitory activity of some Amaryllidaceae alkaloids and Narcissus extracts. *Life Sci* 71(21), 2521-2529.
- Maelicke, A., Samochocki, M., Jostock, R., Fehrenbacher, A., Ludwig, J., Albuquerque, E.X., Zerlin, M., 2001. Allosteric sensitization of nicotinic receptors by galantamine, a new treatment strategy for Alzheimer's disease. *Biol Psychiatry* 49(3), 279-288.
- Mahomoodally, M.F., Sadeer, N.B., Suroowan, S., Jugreet, S., Lobine, D., Rengasamy, K.R.R., 2020. Ethnomedicinal, phytochemistry, toxicity and pharmacological benefits of poison bulb – *Crinum asiaticum* L. *S Afr J Bot* 00, 1-14.
- Malarkey, D.E., Johnson, K., Ryan, L., Boorman, G., Maronpot, R.R., 2005. New insights into functional aspects of liver morphology. *Toxicol Pathol* 33(1), 27-34.

- McGill, M.R., Jaeschke, H., 2019. Animal models of drug-induced liver injury. *Biochim Biophys Acta Mol Basis Dis* 1865(5), 1031-1039.
- Min, B.S., Gao, J.J., Nakamura, N., Kim, Y.H., Hattori, M., 2001. Cytotoxic alkaloids and a flavan from the bulbs of *Crinum asiaticum* var. *japonicum*. *Chem Pharm Bull (Tokyo)* 49(9), 1217-1219.
- Pandit, A., Sachdeva, T., Bafna, P., 2012. Drug-Induced Hepatotoxicity: A Review. *J Appl Pharm Sci* 02(05), 233-243.
- Park, M.H., 2000. Chemical Constituents and Biological Activity of *Crinum asiaticum* var. *japonicum*. Graduated School of Chungnam National University for the degree of Master of Pharmaceutical Science.
- Pettit, G.R., Cragg, G.M., Singh, S.B., Duke, J.A., Doubek, D.L., 1990. Antineoplastic agents, 162. *Zephyranthes candida*. *J Nat Prod* 53(1), 176-178.
- Recknagel, R.O., Glende, E.A., Dolak, J.A., Waller, R.L., 1989. Mechanisms of carbon tetrachloride toxicity. *Pharmacol Ther* 43(1), 139-154.
- Refaat J, M.S.K., Mahmoud A.R., Ahmed A.A., 2013. *Crinum*; An endless source of bioactive principles; A review. Part V. Biological Profile. *IJPSR* 4(4), 1239-1252.

- Roy, A., Bhoumik, D., Sahu, R.K., Dwivedi, J., 2014. Medicinal plants used in liver protection-a review. UK J Pharm Biosci 2(1), 23-33.
- Roy, M., Liang, L., Xiao, X., Feng, P., Ye, M., Liu, J., 2018. Lycorine: A prospective natural lead for anticancer drug discovery. Biomed Pharmacother 107, 615-624.
- Samud, A.M., Asmawi, M.Z., Sharma, J.N., Yusof, A.P., 1999. Anti-inflammatory activity of *Crinum asiaticum* plant and its effect on bradykinin-induced contractions on isolated uterus. Immunopharmacology 43(2-3), 311-316.
- Scholten, D., Trebicka, J., Liedtke, C., Weiskirchen, R., 2015. The carbon tetrachloride model in mice. Lab Anim 49(S1), 4-11.
- Shakya, A.K., 2020. Drug-induced Hepatotoxicity and Hepatoprotective Medicinal Plants: A Review. Indian J Pharm Educ Res 54(2), 234-250.
- Shen, J., Zhang, T., Cheng, Z., Zhu, N., Wang, H., Lin, L., Wang, Z., Yi, H., Hu, M., 2018. Lycorine inhibits glioblastoma multiforme growth through EGFR suppression. J Exp Clin Cancer Res 37(1), 157.
- Singh, K.A., Nayak, M.K., Jagannadham, M.V., Dash, D., 2011. Thrombolytic along with anti-platelet activity of crinum, a protein constituent of *Crinum asiaticum*. Blood Cells Mol Dis 47(2), 129-132.

- Solis-Herruzo, J.A., De La Torre, P., Munoz-Yague, M.T., 2003. Hepatic stellate cells (HSC): architects of hepatic fibrosis. *Rev Esp Enferm Dig* 95(6), 438-439.
- Starkel, P., Leclercq, I.A., 2011. Animal models for the study of hepatic fibrosis. *Best Pract Res Clin Gastroenterol* 25(2), 319-333.
- Tan, C.X., Schrader, K.K., Mizuno, C.S., Rimando, A.M., 2011. Activity of lycorine analogues against the fish bacterial pathogen *Flavobacterium columnare*. *J Agric Food Chem* 59(11), 5977-5985.
- Treuting, P.M., Dintzis, S.M., Montine, K.S., 2017. Comparative anatomy and histology: a mouse, rat, and human atlas. Academic Press Second Edition, 229-239.
- Vrijssen, R., Berghe, D.V., Vlietinck, A. Boeye, A., 1986. Lycorine: a eukaryotic termination inhibitor? *J Biol Chem* 261(2), 505-507.
- Wang, G., Huang, K., Dong, Y., Chen, S., Zhang, J., Wang, J., Xie, Z., Lin, X., Fang, X., Fan, S., 2018. Lycorine Suppresses Endplate-Chondrocyte Degeneration and Prevents Intervertebral Disc Degeneration by Inhibiting NF-kappaB Signalling Pathway. *Cell Physiol Biochem* 45(3), 1252-1269.
- Wang, H., Liang, X., Gravot, G., Thorling, C., Crawford, D., Xu, Z., Liu, X., Roberts, M., 2017. Visualizing liver anatomy, physiology and pharmacology using multiphoton microscopy. *J Biophotonics* 10(1), 46-60.

- Weniger, B., Italiano, L., Beck, J.P., Bastida, J., Bergonon, S., Codina, C., Lobstein, A., Anto, R., 1995. Cytotoxic activity of Amaryllidaceae alkaloids. *Planta Med* 61(1), 77-79.
- Wu, S., Qiu, Y., Shao, Y., Yin, S., Wang, R., Pang, X., Ma, J., Zhang, C., Wu, B., Koo, S., Han, L., Zhang, Y, Gao, X., Wang, T., Yu, H., 2018. Lycorine Displays Potent Antitumor Efficacy in Colon Carcinoma by Targeting STAT3. *Front Pharmacol* 9, 881.
- Yoon, H.S., Kagn, J.I., Kim, S.M., Ko, A., Koh, Y.S., Hyun, J.W., Yoon, S.P., Ahn, M., Kim, Y.H., Kang, J.H., 2019. Norgalanthamine stimulates proliferation of dermal papilla cells via anagen-activating signaling pathways. *Biol Pharm Bull* 42(1), 139-143.
- Zhao, J., Tang, N., Wu, K., Dai, W., Ye, C., Shi, J., Zhang, J., Ning, B., Zeng, X., Lin, Y., 2014. MiR-21 simultaneously regulates ERK1 signaling in HSC activation and hepatocyte EMT in hepatic fibrosis. *PLoS One* 9(10), e108005, 1-10.

**Hepatoprotective effects of norgalanthamine on
carbon tetrachloride (CCl₄)-induced liver injury
in mice**

1. Abstract

Norgalanthamine is a major component of *Crinum asiaticum* var. *japonicum* that exhibits several biological activities. This study evaluated the anti-inflammatory and anti-oxidative properties of norgalanthamine in mice with carbon tetrachloride (CCl₄)-induced acute liver injury. Norgalanthamine (1 and 10 mg/kg) was orally administered to mice for 7 days, after which liver injury was induced by CCl₄ (1.5 ml/kg, i.p.). The vehicle and positive controls consisted of phosphate-buffered saline and silymarin (100 mg/kg), respectively. The mice were euthanized 24 h after CCl₄ administration.

In CCl₄-injured mice, norgalanthamine pretreatment significantly reversed the increases in serum alanine aminotransferase, aspartate aminotransferase, and total bilirubin levels, and the decrease in the serum glucose level. In the liver, norgalanthamine restored the activities of the antioxidant enzymes superoxide dismutase and catalase, while reducing lipid accumulation and, concurrently, the expression of genes involved in lipid synthesis, including peroxisome proliferator-activated receptor γ and adipocyte protein-2. Norgalanthamine also ameliorated inflammation by down-regulating the expression of the pro-inflammatory mediators TNF- α , IL-1 β , and MCP-1, and up-regulating the Nrf2/HO-1 pathway. The hepatoprotective effect of norgalanthamine in CCl₄-injured mice was also reflected in the histopathologic scores. In addition, norgalanthamine decreased collagen deposition in liver tissue as shown on picrosirius red staining by down-regulating expression of the fibrosis-related genes α SMA and fibronectin. The findings indicate that norgalanthamine attenuates liver fibrosis and could be a novel approach in its prevention.

Collectively, these findings imply that norgalanthamine mitigates CCl₄-induced hepatic injury by increasing anti-oxidative activity, down-regulating pro-inflammatory mediators and fibrosis-related genes in the liver.

Key words: Norgalanthamine; fibrosis; inflammation; steatosis.

2. Introduction

Carbon tetrachloride (CCl₄) is a hepatotoxic substance that is used in animal models of liver injury characterized by centrilobular hepatic necrosis (Ahn *et al.*, 2014; Cao *et al.*, 2017; Li *et al.*, 2016; Rahman and Hodgson, 2000; Recknagel *et al.*, 1989), as well as pathophysiological changes, fatty changes (Unsal *et al.*, 2020), inflammation, and fibrosis (Scholten *et al.*, 2015; Unsal *et al.*, 2020). CCl₄ injury results from direct damage to tissue after injection and metabolism. CCl₄ is converted to trichloromethyl radicals (CCl₃^{*}) by cytochrome P450 (CYP), especially CYP2E1, CYP2B1, CYP2B2, and CYP3A (Kim *et al.*, 2010; Scholten *et al.*, 2015). The CCl₄ model of liver injury has been widely used to evaluate the therapeutic potential of drugs aimed at treating liver disease, and to study xenobiotic-induced liver injury, which resembles human liver disease both morphologically and in terms of the biochemical features of the cellular lesions (McGill and Jaeschke, 2019; Scholten *et al.*, 2015). CCl₄ induces hepatotoxicity after metabolite activation in the liver (McGill and Jaeschke, 2019; Scholten *et al.*, 2015). The initial response to CCl₄ consists of the activation of hepatic macrophages, including Kupffer cells, the generation of free radicals, and the production of inflammatory mediators, including the cytokine tumor necrosis factor-alpha (TNF- α) and interleukins (ILs) (Bansal *et al.*, 2005; Decker, 1990; Munakarmi *et al.*, 2020; Zou *et al.*, 2016), chemokines such as monocyte chemoattractant protein (MCP)-1 (Russmann *et al.*, 2009), and pro-inflammatory mediators such as inducible nitric oxide synthase and cyclooxygenase, via the activation of nuclear factor kappa B (Liu *et al.*, 2018a; Wu *et al.*, 2018). Therefore, the CCl₄-injured liver has been used to test the efficacy of anti-inflammatory agents (Badger *et al.*, 1996; Liu *et al.*, 2018b; Ma *et al.*, 2015; Rocha *et al.*, 2014; Son *et al.*, 2007; Tipoe *et al.*, 2010), with a particular focus on therapies based on a single compound (Ahn *et al.*, 2014; Hansen *et al.*, 2017; Kim *et al.*, 2010; Munakarmi *et al.*, 2020; Vargas-Mendoza *et al.*, 2014; Yang *et al.*, 2015; Zou *et al.*, 2016).

Norgalanthamine, a major component of *Crinum asiaticum* var. *japonicum*, is a metabolite of galanthamine, a selective acetylcholinesterase inhibitor that promotes hair growth via the proliferation of dermal papilla, activation of the ERK 1/2, PI3K/AKT, and Wnt/ β -catenin pathways (Yoon *et al.*, 2019), and inhibition of 5 α -reductase activity and of the TGF- β 1-induced canonical pathway (Kang *et al.*, 2017). In this study, we investigated the hepatoprotective effects of norgalanthamine in the context of its effects on biochemical indicators of liver damage, the activities of oxidative stress enzymes, and the levels of inflammatory mediators.

3. MATERIALS AND METHODS

Chemical and reagents

Norgalanthamine (D292035) was obtained from Toronto Research Chemicals (Toronto, Canada). Silymarin, used as a positive control, was purchased from Sigma-Aldrich (St. Louis, MO, USA). Commercial colorimetric assay kits for the measurement of superoxide dismutase (SOD) and catalase (CAT) activity were purchased from Abcam (Cambridge, UK). Polyclonal antibodies targeting Nrf-2 and HO-1 were purchased from Cell Signaling Technology (Beverly, MA, USA), and ionized calcium binding adapter molecule 1 (Iba-1) was provided by Wako Pure Chemical Industries, Ltd. (Osaka, Japan). The ABC Elite kit and diaminobenzidine (DAB) substrate were purchased from Vector Laboratories (Burlingame, CA, USA).

Animals

Six-week-old male C57BL/6 mice weighing 20–22 g (DBL, Chungbuk, Korea) were used for all experiments. The animals were maintained at a controlled temperature of 25–28°C with a 12-h light/dark cycle, fed a standard diet and provided water *ad libitum*. All experimental procedures were conducted in accordance with the guidelines for the Care and Use of Laboratory Animals of Sangji University in Wonju City, Korea (permit number: 2020-11). The animal protocols conformed to current international laws and to the policies of the National Institutes of Health (NIH) Guide for the Care and Use of Laboratory Animals (NIH Publication no. 85–23, 1985, revised 1996). Every effort was made to minimize the number of animals used in this study and to reduce their pain and suffering.

Experimental design

In the acute model, the mice were randomly divided into five groups of six animals each. The norgalanthamine-treated CCl₄-injured group was orally administered norgalanthamine (1 or 10 mg/mL [NG1 and NG10, respectively], diluted in phosphate-buffered saline [PBS], pH 7.4) for 7 consecutive days. In both the acute and chronic models, PBS, which served as the vehicle control and silymarin served as the positive control (100 mg/kg; (Ni and Wang, 2016)). Both were administered following the same protocol. Liver injury was induced with a 1:1 (v/v) mixture of CCl₄ and sterile olive oil injected intraperitoneally (i.p., 1.5 mL/kg). CCl₄ was given once 24 h after the last dose of test substance. In the chronic model, the mice were randomly divided into four groups of six animals each. PBS (pH 7.4) was administered orally to normal controls. The norgalanthamine-treated CCl₄-injured group was orally administered norgalanthamine (10 mg/mL [NG10], diluted in PBS, pH 7.4) for 14 consecutive days. To induce liver injury, a 1:1 (v/v) mixture of CCl₄ and sterile olive oil was injected intraperitoneally (i.p., 1.5 mL/kg). CCl₄ was given every 72 h for 14 days (Ahn *et al.*, 2014) (Fig. 3).

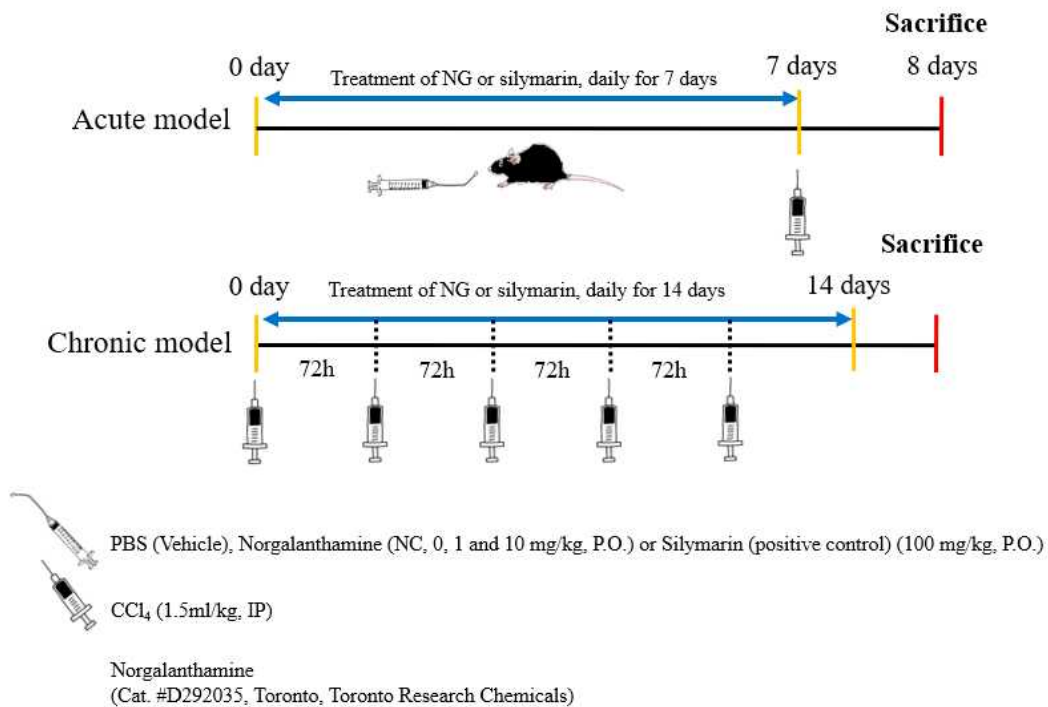


Figure 3. Schematic drawing of the experimental design used to evaluate the effects of norgalanthamine on CCl₄-induced liver injury in mice. Acute model (top), the norgalanthamine-treated CCl₄-injured group was orally administered norgalanthamine (1 or 10 mg/mL [NG1 and NG10, respectively], diluted in phosphate-buffered saline [PBS], pH 7.4) for 7 consecutive days. CCl₄ was given once (i.p., 1.5 mL/kg) 24 h after the last dose of test substance. Chronic model (bottom), the norgalanthamine-treated CCl₄-injured group was orally administered norgalanthamine (10 mg/mL [NG10], diluted in PBS, pH 7.4) for 14 consecutive days. CCl₄ was given every 72 h for 14 days (i.p., 1.5 mL/kg). In both the acute and chronic models, PBS, which served as the vehicle control and silymarin served as the positive control (100 mg/kg).

Sample collection and blood biochemistry analysis

The mice were fasted after treatment and euthanized 24 h after induction of CCl₄ injury in the acute model, or the last dose of the drug in the chronic model. After anesthetization of the mice by isoflurane inhalation (Hana Pharm Co., Ltd, Seoul, Korea), blood was collected from the inferior vena cava for serum analysis the liver was dissected for histopathology, gene expression, and immunochemistry studies (Fig. 3). Liver pieces were fixed in 10% neutral buffered formalin for histopathology or immediately frozen and stored for RNA extraction. Blood samples were centrifuged at 13,000 rpm for 10 min at 4°C to separate the serum. The serum levels of alanine aminotransferase (ALT), aspartate aminotransferase (AST), total bilirubin (T-bil), and glucose were measured using a Beckman Coulter AU680 analyzer (Beckman Coulter, Tokyo, Japan) according to the manufacturer's instructions.

Histopathological examination of liver damage

Sections (4 μm) of paraffin-embedded liver were deparaffinized and then stained with hematoxylin and eosin (H&E) for light microscopy examination. The degree of necrosis after acute liver injury was evaluated using an injury score based on the severity of necrotic lesions in the liver parenchyma (Table 3). In brief, each sample was independently scored by three pathologists blinded to the group assignment. The scoring system was as follows: grade 0, no pathological change; grade 1, degenerated hepatocytes with rare foci of necrosis; grade 2, small areas of mild centrilobular necrosis around the central vein; grade 3, mild centrilobular necrosis, but more severe than grade 2; grade 4, centrilobular necrosis more severe than grade 3 (Dai *et al.*, 2018; Li *et al.*, 2013).

Necrotic areas were evaluated in paraffin-embedded sections stained with toluidine blue, and the severity of fatty changes was assessed in fixed frozen sections stained with oil red O, which detects neutral triglycerides and lipids. Picrosirius red (Polysciences, Inc., PA, USA) staining was used for fibrillary collagen . The proportions of lipid (red-stained area as a percentage of the total area of the liver section), necrotic (light-blue-stained area as a percentage of the total area of the liver section) area, and collagen deposition (red-stained area as a percentage of the total area of the liver section) were determined using Aperio eSlide Manager software (Leica Biosystems, Buffalo Grove, IL, USA).

Table 3. Grading score for Acute liver injury³⁾

Grade	Criteria
0	No pathological change
1	Presence of degenerated hepatocytes with only rare foci of necrosis
2	Small area of mild centrilobular necrosis a round the central vein
3	Area of mild centrilobular necrosis severer than Grade 2
4	Centrilobular necrosis severer than Grade 3

³⁾ cited by Dai et al., 2018; Li et al., 2013

Assays of antioxidant enzyme activities in liver

Liver pieces from the mice were immediately frozen until use. The tissue was then homogenized in a pestle homogenizer, and SOD and CAT activities were determined according to the instructions supplied with the commercial assay kits (Abcam).

Western blot analysis

Protein expression was analyzed quantitatively by western blot, performed as described in a previous study (Kim *et al.*, 2017). The cytosolic and nuclear fractions were separated using NE-PER® nuclear and cytoplasmic extraction reagents, as recommended by the manufacturer (Thermo Scientific, Rockford, IL, USA). Proteins (40 µg/sample) were subjected to 10% (w/v) sodium dodecyl sulfate or sodium lauryl sulfate polyacrylamide gel electrophoresis (SDS- and SLS-PAGE, respectively) and transferred to a nitrocellulose membrane (Schleicher and Schuell, Keene, NH, USA).

Target proteins were immunodetected by incubation of the membrane for 2 h with specific primary antibodies (Table 4). The bound proteins were detected using a chemiluminescent substrate (Miracle-Star; iNtRON Biotech, Gyeonggi, Korea). The blots were then imaged and the densities of the bands were analyzed using ImageJ software (NIH, Bethesda, MD, USA). β -actin served as the internal control.

The optical density (OD; per mm²) of each band was measured and the density ratios relative to the β -actin band were determined using ImageJ. The data are presented as the means \pm standard error of the mean (SEM).

Table 4. Primary antibodies used in the present study

Antigen	Species, antibody type, manufacturer	Concentration
Iba-1	Rabbit, polyclonal, Wako Pure Chemical Industries (019-19741)	250ng/ml
HO-1	Mouse, monoclonal, Santa Cruz Biotechnology (sc-136960)	200ng/ml
Nrf-2	Rabbit, polyclonal, Santa Cruz Biotechnology (sc-13032)	200ng/ml
β -actin	Mouse, monoclonal Sigma Aldrich (A-1978)	500ng/ml

Abbreviations: HO-1, hemeoxygenase-1; Iba-1, Ionized calcium binding protein-1; IgG, immunoglobulin; Nrf-2, nuclear factor erythroid 2-related factor-2.

Quantitative real-time PCR

Gene-expression levels were analyzed in mRNA extracted from mouse liver using TRIzol® reagent (Ambion, Austin, TX, USA), CellScript™ all-in-one 5× first-strand cDNA, and cDNA Synthesis Master Mix (CellSafe, Gyeonggi-do, Korea). Real-time PCR was performed using Luna® Universal qPCR Master Mix (New England BioLabs, Ipswich, MA, USA). mRNA expression levels were calculated according to the $2^{-\Delta\Delta Ct}$ method, with GAPDH as the internal control. The primers used in the PCRs are listed in Table 3 (Gavish *et al.*, 2008; Nelson *et al.*, 2004; Tipoe *et al.*, 2010; Truong *et al.*, 2016).

Table 5. Primer sequences used in the present study

Primer		Sequence
α -SMA	Sense	5'- GTCCCAGACATCAGGGAGTAA-3'
	Antisense	5'- TCGGATACTTCAGCGTCAGGA-3'
AP-2	Sense	5'- CCGCAGACGACAGGA-3'
	Antisense	5'- CTCATGCCCTTTCATAAACT -3'
CYP1A2	Sense	5'- AGTACATCTCCTTAGCCCCAG-3'
	Antisense	5'- GGTCCGGGTGGATTCTTCAG-3'
CYP2E1	Sense	5'- CGTTGCCTTGCTTGTCTGGA-3'
	Antisense	5'- AAGAAAGGAATTGGGAAAGGTCC-3'
Fibronectin	forward	5'- CGAAGAGCCCTTACAGTTCC-3'
	reverse	5'- CCGTGTAAGGGTCAAAGCAT-3'
IL-1 β	Sense	5'- AGGGCTGCTTCCAAACCTTTGAC -3'
	Antisense	5'- ATACTGCCTGCCTGAAGCTCTTGT -3'
MCP-1	Sense	5'- AGGTCCCTGTCATGCTTCTG-3'
	Antisense	5'- GCTGCTGGTGATCCTCTTGT-3'
PPAR γ	Sense	5'- CAAGAATACCAAAGTGCGATCAA-3'
	Antisense	5'- GAGCAGGGTCTTTTCAGAATAATAAG-3'
TNF- α	Sense	5'- GAGTGACAAGCCTGTAGCCCA -3'
	Antisense	5'- CCC TTC TCC AGC TGG AAG A -3'

Immunohistochemistry

The liver sections were incubated with rabbit anti-Iba-1 antibody. The peroxidase reaction was visualized using a DAB kit (Vector Laboratories, Burlingame, CA, USA). The slides were counterstained with hematoxylin and then mounted. Iba-1-immunostained areas were semi-quantitatively analyzed using ImageJ (n=6 animals per group). Five different sections from each liver were assessed and the positive area was calculated as a percentage of the total area of each section (n=5 animals per group).

Measurement of liver hydroxyproline content

Hepatic hydroxyproline content was quantified colorimetrically in flash frozen liver samples using a hydroxyproline kit (Abcam, Cambridge, UK) according to the manufacturer's instructions. The experimental results were quantified by comparison to a standard curve of known hydroxyproline concentrations and expressed as mg hydroxyproline/mg liver.

Statistical analysis

All results are presented as the means \pm SEM. Statistical significance was defined as a P value < 0.05 based on the results of one-way analysis of variance followed by Bonferroni's multiple comparison post-hoc test.

4. Results

Evaluation of biochemical parameters in serum

Serum levels of the enzymes ALT, AST, and T-bil were measured to determine the protective role of norgalanthamine against CCl₄-induced hepatic injury (Fig. 4). In the control mice, serum ALT, AST and T-bil levels were in the normal range (31.8 ± 2.20 , 42.2 ± 2.29 , and 0.17 ± 0.00 U/L, respectively; Fig. 4) whereas they were significantly higher in the vehicle-treated CCl₄-injured mice ($6,088.0 \pm 697.47$ U/L, $p < 0.001$) mice they were significantly higher than in the normal control mice (0.27 ± 0.02 U/L).

Pretreatment with 1 mg norgalanthamine/kg significantly reduced levels of ALT ($4,176.0 \pm 441.97$ U/L, $p < 0.05$) and AST ($2,952.0 \pm 358.07$ U/L, $p < 0.05$) in mice with CCl₄-induced liver injury. At the higher dose of 10 mg norgalanthamine/kg, significant dose-dependent reductions compared to vehicle-treated CCl₄-injured mice were determined for ALT ($3,588.00 \pm 281.13$ U/L, $p < 0.01$), AST ($2,236.00 \pm 158.83$ U/L, $p < 0.001$), and T-bil (0.22 ± 0.01 U/L, $p < 0.05$).

In the positive control (silymarin 100), serum ALT ($3,588.00 \pm 225.73$ U/L, $p < 0.01$), AST ($1,840.00 \pm 185.66$ U/L, $p < 0.001$), and T-bil (0.21 ± 0.01 U/L, $p < 0.05$) levels decreased significantly compared to the vehicle-treated mice. The absence of a significant difference between the silymarin and norgalanthamine groups implies that the effects on serum biomarkers of CCl₄-induced liver injury were similar.

Serum glucose levels were also measured and found to be significantly lower in the vehicle-treated mice (32.80 ± 3.53 U/L) than in the normal control mice

(296.60 ± 17.87 U/L, $p < 0.001$), but significantly higher in NG10 mice (104.40 ± 6.95 U/L) than in vehicle-treated mice (32.80 ± 3.53 U/L, $p < 0.05$).

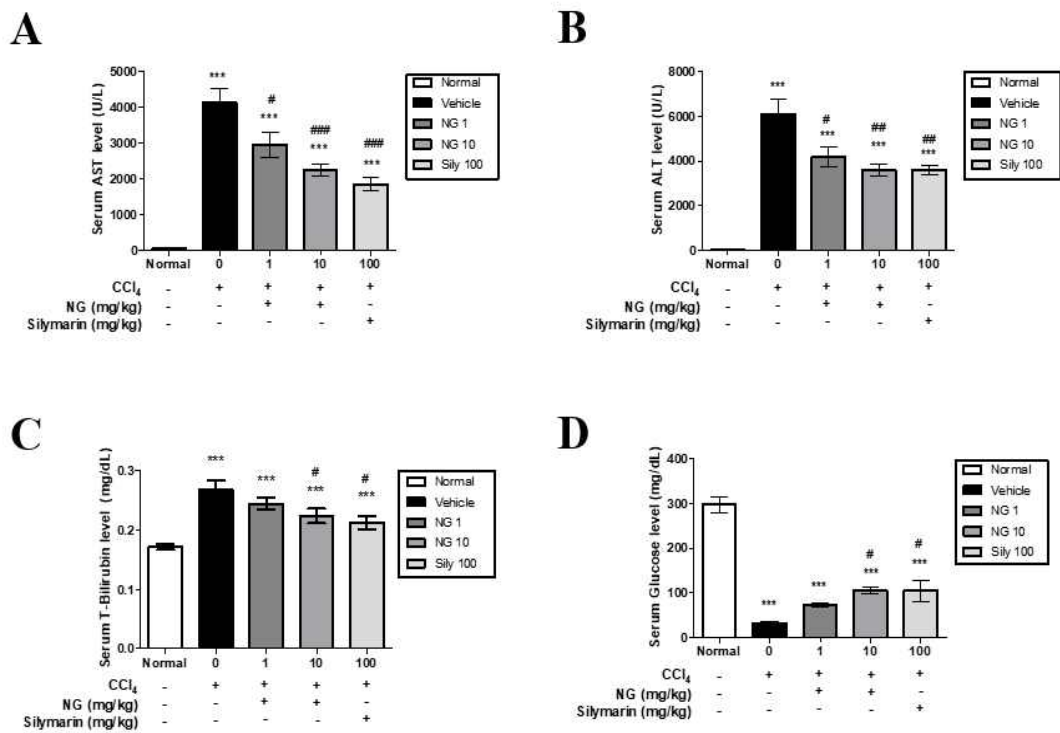


Figure 4. The effects of norgalanthamine on the serum levels of biochemical parameters in mice with CCl₄-induced acute liver injury. (A) The inhibitory effects of norgalanthamine (1 and 10 mg/kg) on serum aspartate aminotransferase (AST), (B) alanine aminotransferase (ALT), (C) total bilirubin, and (D) glucose in mice with CCl₄-induced acute liver injury. Silymarin (positive control) dose: 100 mg/kg. Values are mean \pm SEM, n = 5 per group. *** $P < 0.001$ vs. normal control; # $P < 0.05$, ## $P < 0.01$, ### $P < 0.001$ vs. CCl₄-induced acute injury with vehicle treatment.

Norgalanthamine improves histopathological changes in the liver

The histopathological studies demonstrated protective effects of norgalanthamine against CCl₄-induced liver injury (Fig. 5). In the normal control mice, the liver showed a normal histological architecture, including hepatic cells with well-preserved cytoplasm, a prominent nucleus, and a central vein (Fig. 5A). In the livers of CCl₄-induced mice, however, large areas of pericentral necrosis were seen together with a loss of hepatic architecture, an inflammatory cell infiltrate, and cell swelling (Fig. 5B). The hepatic lesions were less severe in the livers of the NG1, NG10, and silymarin 100 CCl₄-injured mice (Fig. 5C, 5D) than in those of the vehicle-treated CCl₄ control mice (Fig. 5E).

Liver-injury grades were evaluated based on H&E staining. Based on the histological scores, pretreatment with either 1 or 10 mg norgalanthamine significantly inhibited acute hepatic injury compared to vehicle treatment ($p < 0.001$). Similar effects were observed in the silymarin 100 group (Fig. 5F).

The extent of centrilobular necrosis around the central vein was assessed by toluidine blue staining (Fig. 5G). The semi-quantitative results showed a larger necrotic area in the vehicle-treated CCl₄ control group, but a reduction in the extent of necrosis was seen in the NG10 and silymarin 100 groups.

The liver tissue of the mice was also examined for fatty changes (Fig. 6). In the normal control, lipid droplets were not detected by oil red O staining (Fig. 6A), whereas in the vehicle-treated CCl₄-injured group staining revealed diffuse fatty degeneration throughout the liver (Fig. 6B). By contrast, in the NG1 and NG10 groups (Fig. 6C, 6D), and in the silymarin 100 group (Fig. 6E), there was a relative reduction in the extent of fatty changes in the livers of mice with CCl₄-induced

injury. The percentage of oil-red-O-positive areas was significantly higher in the vehicle-treated group than in the normal control group ($p < 0.001$), but was significantly reduced in the NG1 and NG10 groups ($p < 0.001$), as well as the silymarin 100 group ($p < 0.001$) (Fig. 6F). These results imply that norgalanthamine treatment can mitigate CCl_4 -induced histopathological changes in mouse liver.

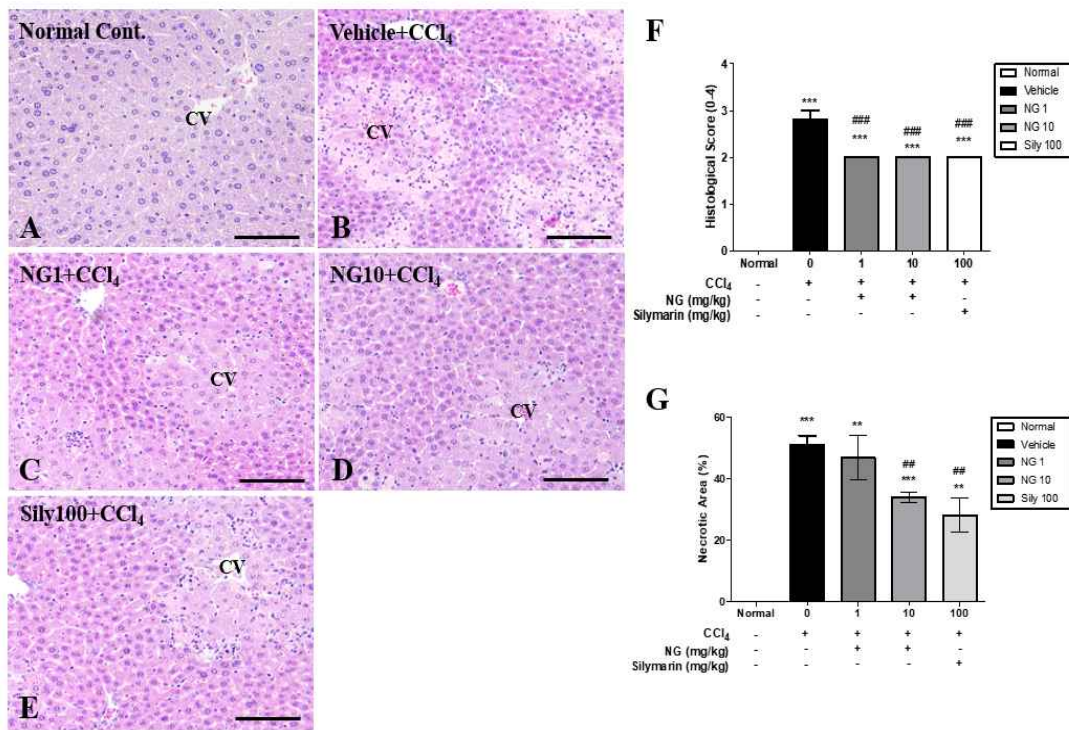


Figure 5. Protective effects of norgalanthamine on the histology of the liver in mice with CCl₄-induced acute liver injury. Liver tissues were stained with hematoxylin and eosin (H&E) and their histological characteristics were assessed by three blinded observers. (A) Normal control group; (B) CCl₄ vehicle group; (C) CCl₄ injury + 1 mg norgalanthamine /kg; (D) CCl₄ injury + 10 mg norgalanthamine/kg; (E) CCl₄ injury + 100 mg silymarin/kg; (F), histological score (0–4); (G) quantitative analysis of toluidine blue-negative areas in mouse liver. Values represent mean ± SEM, n = 5 per group. ** p<0.01 and *** p<0.001 vs. normal control group; ## p<0.01 and ### p<0.001 vs. CCl₄-induced acute injury with vehicle treatment. Scale bar = 100 μm.

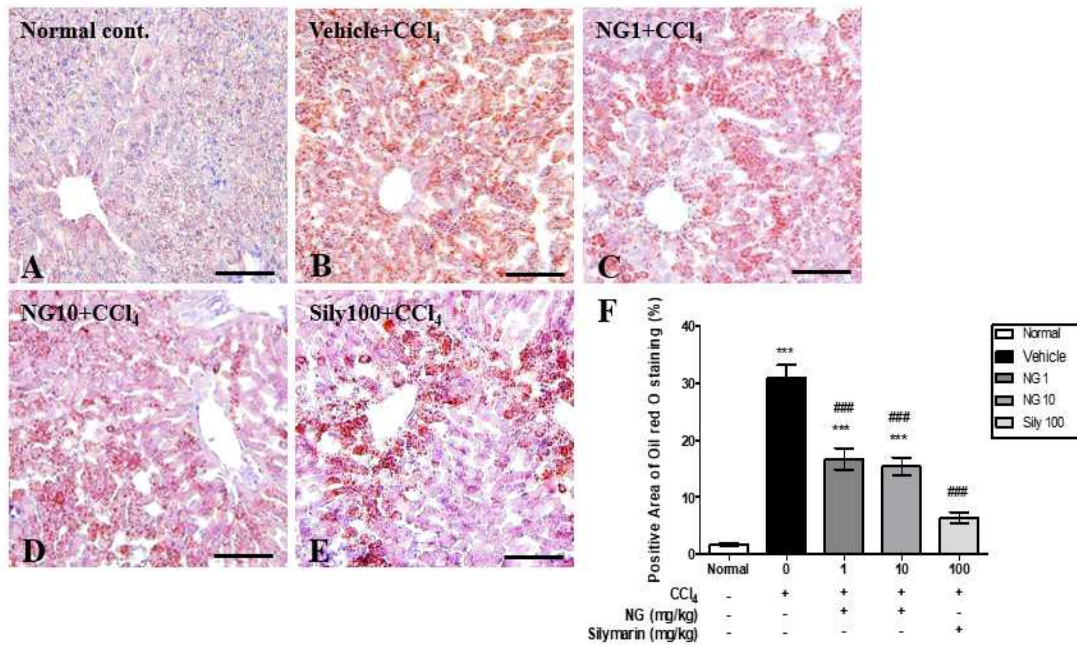


Figure 6. Oil red O staining of frozen sections of liver tissue from treated and untreated mice reveals lipid accumulation. (A) Normal control; (B), CCl₄-induced vehicle-treated group; (C), CCl₄ injury +1 mg norgalanthamine/kg; (D) CCl₄ injury +10 mg norgalanthamine/kg; (E) positive control: CCl₄ injury +100 mg silymarin/kg; (F) quantification of oil-red-O-positive areas. Values represent means ± SEM, n = 5 per group. *** P < 0.001 vs. normal control; ### P < 0.001 vs. CCl₄-induced acute injury with vehicle treatment. Scale bar = 100 μm.

Norgalanthamine regulation of expression of hepatic CYP1A2 gene

The hepatic mRNA expression of CYP1A2 and CYP2E1 was determined by qPCR analysis (Fig. 7). CYP2E1 mRNA expression was significantly decreased in all administration groups compared to the normal control group (vehicle-treated CCl₄ group and NG10, $p < 0.01$; NG 1 and silymarin, $p < 0.05$). However, in all the treatment groups, expression levels showed no changes. On the other hand, CYP1A2 mRNA expression significantly decreased in the vehicle-treated CCl₄ group compared to the normal control group, but increased significantly in the NG10 groups ($p < 0.05$) and silymarin ($p < 0.001$) groups.

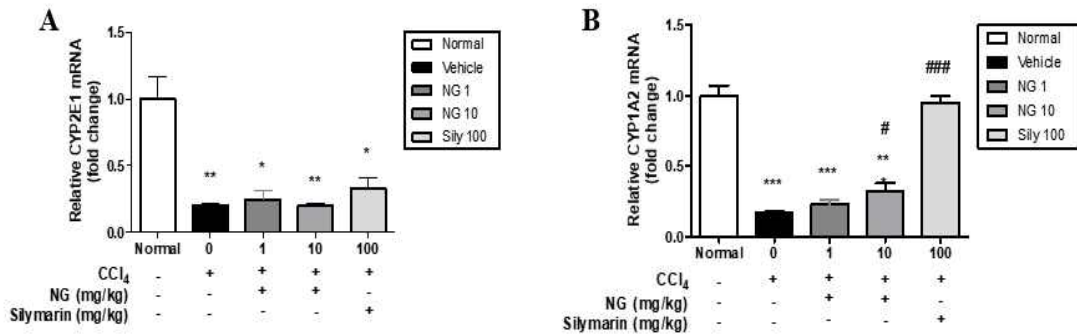


Figure 7. mRNA expression levels of CYPs in the liver (A–B). The mRNA expression levels of CYP2E1 and CYP1A2 were measured using the quantitative reverse transcription polymerase chain reaction. Gapdh was used as the housekeeping gene. The data are presented as the means± SEM. * $p < 0.05$, ** $p < 0.01$ and *** $p < 0.001$ vs. the normal control group; # $p < 0.05$ and ### $p < 0.001$ vs. the CCl₄-induced acute injury group with vehicle treatment. mRNA: messenger RNA; CYPs: Cytochrome P450.

Norgalanthamine up-regulates SOD and catalase activities

The antioxidant effects of norgalanthamine on CCl₄-induced liver injury were investigated by measuring the activities of the antioxidant enzymes SOD and CAT in the liver tissues of the five groups of mice (Fig. 8). In the CCl₄-induced mice, SOD and CAT activities decreased significantly (80.37 ± 5.24 and 0.46 ± 0.04 U/L, respectively; both $p < 0.05$). Pre-treatment with norgalanthamine prior to CCl₄ injury significantly up-regulated the levels of both enzymes compared to the vehicle-treated mice, with a significant effect on SOD seen in the NG10 group (102.22 ± 2.26 U/L, $p < 0.01$; Fig. 8A), and on CAT in both the NG1 and NG10 groups (0.62 ± 0.03 , $p < 0.01$; 0.98 ± 0.21 , $p < 0.05$, respectively; Fig. 8B). This implies that the hepatoprotective effect of norgalanthamine is derived from its antioxidant activity.

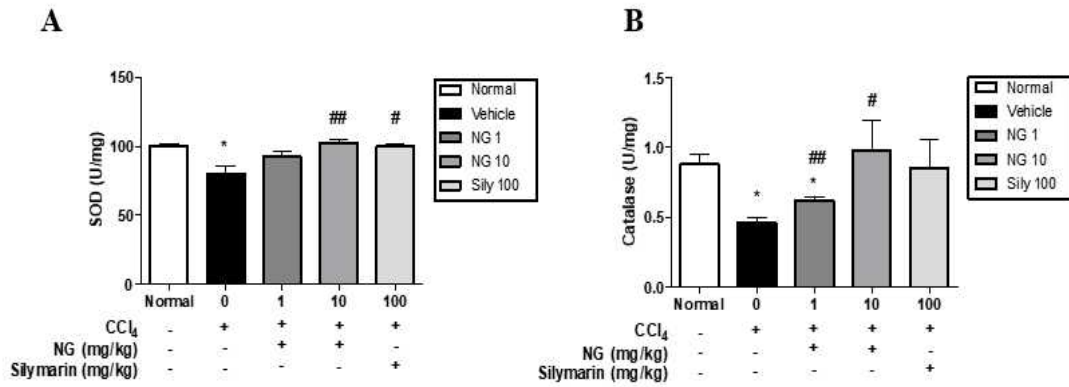


Fig. 8. Antioxidant effect of norgalanthamine in mice with CCl₄-induced acute liver injury. Injury is as indexed by the enzyme activities of (A) superoxide dismutase and (B) catalase. The data are expressed as means \pm SEM, n = 5 per group. * $P < 0.05$ vs. the normal control; # $P < 0.05$ and ## $P < 0.01$ vs. the CCl₄-induced acute injury with vehicle treatment group.

Norgalanthamine reduced inflammation in the liver

The anti-inflammatory properties of norgalanthamine were further evaluated by assessing TNF- α , IL-1 β , and MCP-1 mRNA levels in the livers of the mice (Fig. 9). TNF- α and IL-1 β mRNA expression increased significantly in the vehicle-treated CCl₄-injured group (3.41 ± 0.56 and 2.37 ± 0.27 U/L, respectively) versus the normal control group (0.71 ± 0.26 and 1.42 ± 0.45 U/L, respectively; both $p < 0.01$) but were significantly reduced in the norgalanthamine groups (2.30 ± 0.27 and 1.47 ± 0.02 U/L, respectively, both $p < 0.05$; Fig. 9A, B). In addition, the mRNA levels of the inflammatory chemokine MCP-1 were significantly higher in the vehicle-treated CCl₄-injured group than in the normal control group (12.37 ± 1.00 vs. 1.31 ± 0.27 U/L; $p < 0.01$) and significantly lower in the NG1 and NG10 groups than in the vehicle treatment group (6.36 ± 1.33 -fold change, 6.94 ± 0.77 -fold change, respectively, both $p < 0.01$; Fig. 9).

Kupffer cells/macrophages are activated during liver injury (Ahn *et al.*, 2016). In the mouse livers in the normal control group, Iba-1-positive Kupffer cells were detected along the sinusoids (Fig. 10A), but no infiltration of inflammatory cells was observed. By contrast, in the livers of CCl₄-injured mice, activated Kupffer cells and an inflammatory cell infiltrate were detected (Fig. 10B). Pretreatment with 10 mg norgalanthamine/kg (Fig. 10D) or 100 mg silymarin/kg (Fig. 10E) reduced the numbers of Iba1-positive cells. Furthermore, while the percentages of Iba-1-positive areas were significantly higher in the vehicle-treated group than in the normal control group ($p < 0.01$), they were significantly lower in the NG10 ($p < 0.01$) and silymarin 100 ($p < 0.01$) groups than in the vehicle-treated group (Fig. 10F).

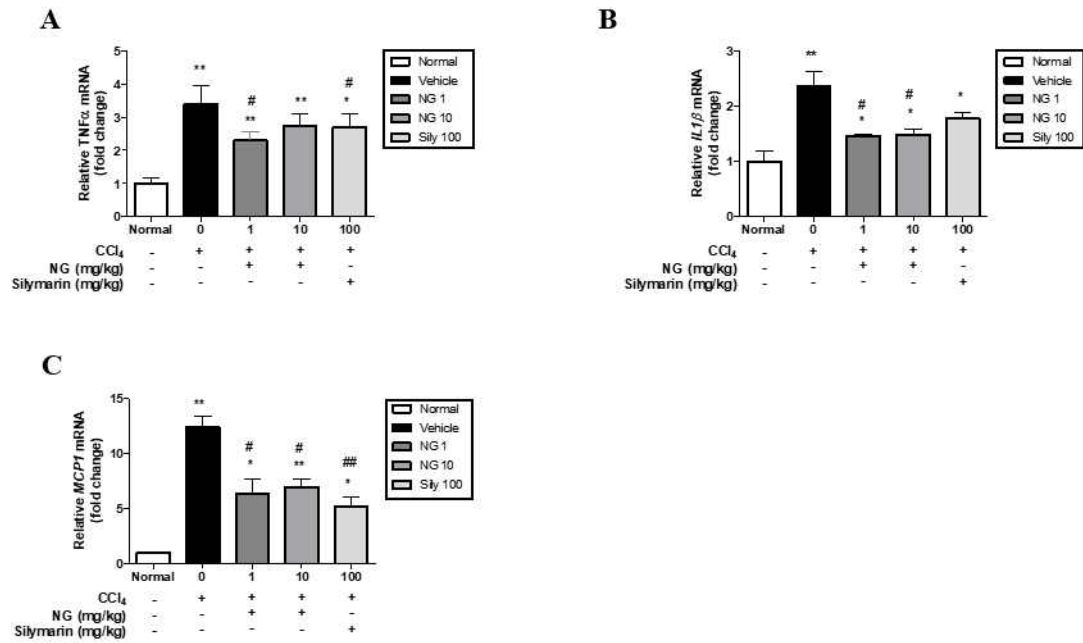


Figure 9. Norgalanthamine pretreatment attenuates CCl₄-induced inflammatory responses in the liver at the transcriptional level. (A) TNF α mRNA; (B), IL1 β mRNA; and (C), MCP-1 mRNA. Data are presented as means \pm SEM, n = 5 per group. * P < 0.05 and ** P < 0.01 vs. the normal control; # P < 0.05 and ## P < 0.01 vs. the CCl₄-induced acute-liver-injury with vehicle treatment group.

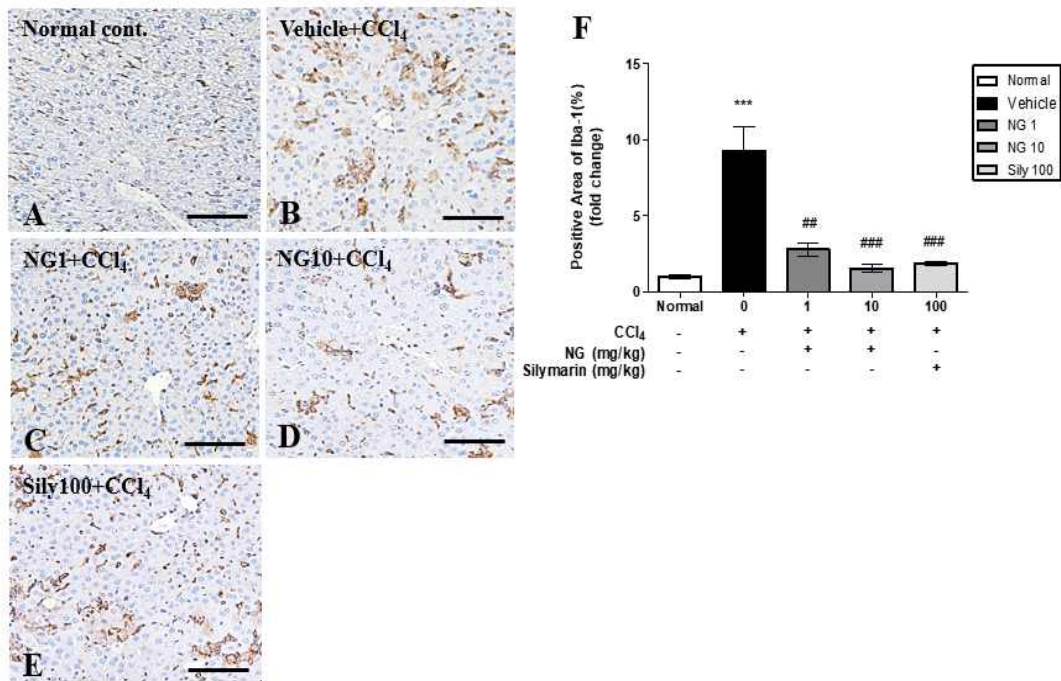


Figure 10. (A–E) Immunohistochemical staining of Iba-1 in liver sections. (F) Bar graph shows the semi-quantitative analysis of Iba-1-positive areas. Scale bar = 100 μ m. Values in (F) are means \pm SEM, n = 5 per group. * $P < 0.001$ vs. the normal control group; ## $P < 0.01$, ### $P < 0.001$ vs. the CCl₄-induced acute-liver-injury with vehicle treatment group.**

Norgalanthamine down-regulates the expression of mRNAs linked to adipogenesis in the liver

The molecular mechanisms underlying the anti-adipogenic effects of norgalanthamine were investigated by analyzing the mRNA levels of genes involved in lipid uptake and metabolism, including proliferator-activated receptor- γ (PPAR- γ) and adipocyte fatty acid-binding protein-2 (AP2) (Fig. 11). The results showed that the two genes were expressed at significantly higher levels in the vehicle-treated group ($p < 0.01$) whereas norgalanthamine treatment caused significant reductions in both genes ($p < 0.05$).

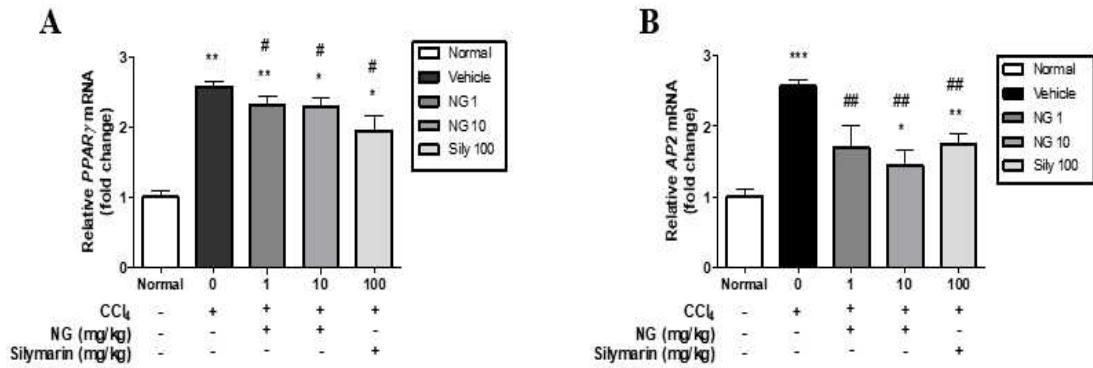


Figure 11. Real-time PCR analyses of PPAR- γ and AP2 expression in liver tissues. Bar graph shows the expression of PPAR- γ and AP2 in CCl₄-induced acute-liver-injury mice relative to that of the normal control mice. Data are presented as means \pm SEM, n = 5 per group. * $P < 0.05$, ** $P < 0.01$ vs. the normal control group; # $P < 0.05$ and # $P < 0.01$ vs. the CCl₄-induced acute injury with vehicle treatment group.

Norgalanthamine up-regulates Nrf-2 and HO-1 levels in mice with CCl₄-induced liver injury

Western blotting was performed to determine the effect of norgalanthamine on Nrf-2 levels in the cytosol and nucleus of liver cells in the treated mice. Compared to the vehicle-treated group, norgalanthamine significantly increased both the cytoplasmic levels of Nrf-2 and the extent of the protein's nuclear translocation (Fig. 12A). Consistent with these findings, HO-1 protein levels were significantly higher in the NG10 group than in the vehicle-treated group (Fig. 12B).

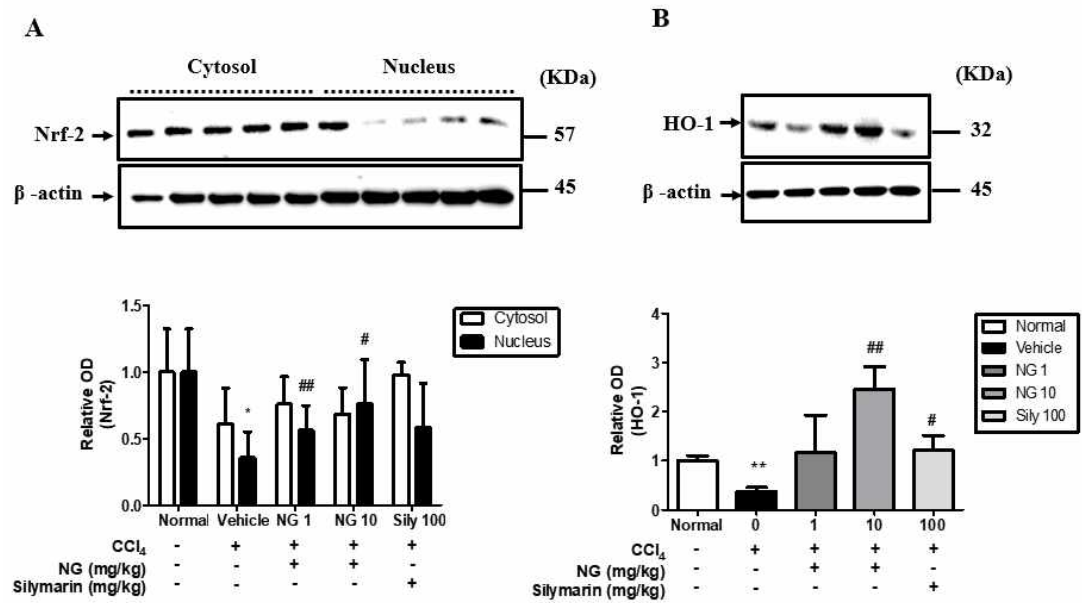


Figure 12. Representative immunoblots of (A) Nrf-2 and HO-1 and (B) Nrf-2 and HO-1 expression relative to the β -actin level in CCl₄-induced acute-liver-injury mice. Data are presented as mean \pm SE, n = 5 per group. * $P < 0.05$ vs. the normal control group; # $P < 0.05$ and # $P < 0.01$ vs. the CCl₄-induced acute injury with vehicle treatment group.

Effects of norgalanthamine on CCl₄-induced chronic liver injury

Liver sections were stained with Picrosirius red stain. Collagen fibers were detected around perivenular regions of the normal control group (Fig. 13A). However, collagen tissue proliferation by fibrosis was detected in the vehicle-treated group (Fig. 13B). The norgalanthamine and silymarin treatments significantly reduced collagen tissue proliferation in the liver (Fig. 13C and 13D) compared with the vehicle-treated group. The positive areas with Picrosirius red staining were significantly higher in the vehicle-treated group ($3.77 \pm 0.27\%$, $p < 0.01$) than in the normal control group ($1.60 \pm 0.14\%$). The 10-mg/kg norgalanthamine group ($3.00 \pm 0.02\%$, $p < 0.05$) showed significantly lower percent areas of collagen tissue compared with the liver tissue in the vehicle-treated group (Fig. 13F). In liver tissue, hydroxyproline levels were significantly lower in the 10-mg/kg norgalanthamine group (189.26 ± 35.53 g, $p < 0.05$) than in the vehicle-treated group (33.87 ± 5.81 g) (Fig. 13G). Changes in the biochemical serum and histopathological parameters of CCl₄-induced chronic-liver-injury mice were similar to those in CCl₄-induced acute-liver-injury mice (data not shown). In addition, the expression of α -SMA and fibronectin mRNA decreased significantly in the 10-mg/kg norgalanthamine group (3.33 ± 1.76 -fold change, $p < 0.01$; 1.03 ± 0.15 -fold change, $p < 0.05$) compared to the vehicle-treated group (5.24 ± 1.75 -fold change; 1.48 ± 0.07 , both $p < 0.05$) (Fig. 14).

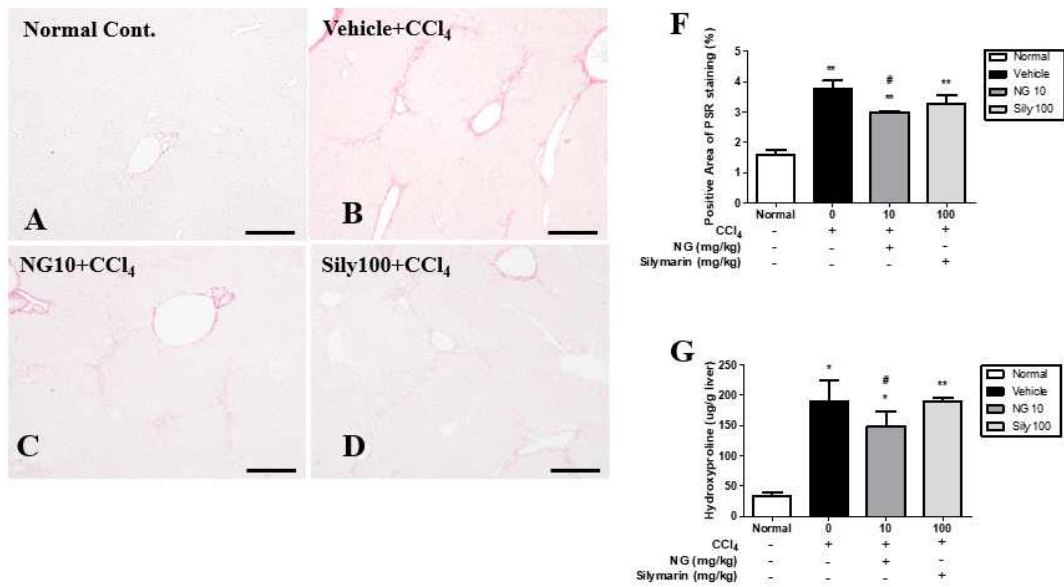


Figure 13. Effects of norgalanthamine in CCl₄-induced chronic liver injury in mice. (A–D) Picrosirius red staining of liver sections. (F) Positive area of Picrosirius red staining. (G) Quantitative hydroxyproline in CCl₄-induced chronic liver injury mice. Data are presented as means ± SEM, n = 5 per group. * $P < 0.05$ and ** $P < 0.01$ vs. the normal control group; # $P < 0.05$ vs. the CCl₄-induced acute injury with vehicle treatment group.

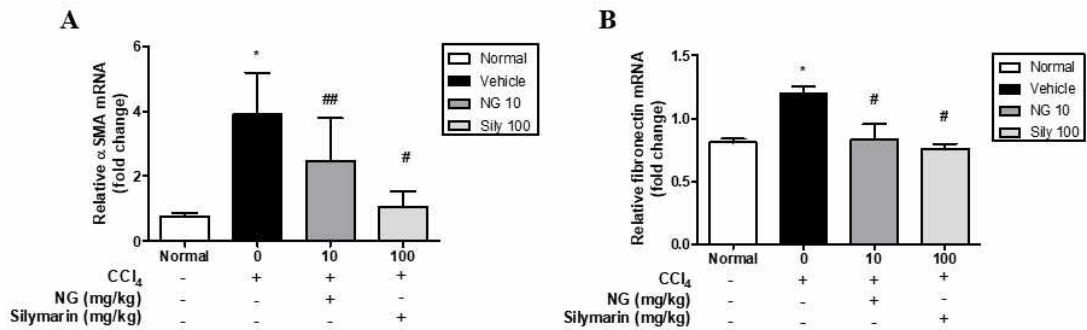


Figure 14. Real-time PCR analyses of α -SMA and fibronectin expression in liver tissues. Bar graph shows the expression of α SMA and fibronectin in CCl₄-induced acute-liver-injury mice relative to that of the normal control group. Data are presented as means \pm SEM, n = 5 per group. * $P < 0.05$ vs. the normal control group; # $P < 0.05$ and ## $P < 0.01$ vs. CCl₄-induced acute-liver-injury with vehicle treatment group.

5. Discussion

This study examined the effects of norgalanthamine, a principal component of *Crinum asiaticum* var. *japonicum*, in CCl₄-induced acute- and chronic-liver-injury models in mice to determine whether norgalanthamine has preventive or therapeutic effects in acute and chronic liver damage. The CCl₄-induced liver-injury model is characterized by excessive accumulation of ROS in hepatocytes or extracellular regions, increased activated inflammatory cells, hepatocellular necrosis, and liver fibrosis, and abnormal levels of liver enzymes in the blood (Ahn *et al.*, 2016; Zeashan *et al.*, 2008). We found that administration of norgalanthamine prior to CCl₄ induction in mice reduced the elevation of serum enzyme levels of ALT, AST, and T-bil, and increased glucose activity in blood serum. These findings imply that norgalanthamine has a preventive effect on hepatocytes in the CCl₄-induced acute-liver-injury model.

The hepatoprotective effect of norgalanthamine was further demonstrated biochemically and histopathologically. The major cause of CCl₄-induced liver injury is thought to be oxidative stress mediated by the free radical derivatives of CCl₄. In this study, the activities of SOD and CAT and expression of Nrf-2 and HO-1 were significantly decreased in mouse liver after CCl₄-induction (Ahn *et al.*, 2016; Singh *et al.*, 2015; Song *et al.*, 2011). Of note, we found that expression was restored to almost normal levels in the norgalanthamine groups. Oxidative stress causes the escape by Nrf-2 of Keap1-mediated proteasomal degradation, leading to Nrf-2 nuclear translocation and binding to ARE (Cao *et al.*, 2017; Kensler *et al.*, 2007). Nrf-2 and its downstream target HO-1, together with other antioxidant enzymes (e.g., SOD and glutathione peroxidase), play important roles in tissue protection, by regulating the expression of cytoprotective and antioxidant genes (Jiang *et al.*, 2016). This study implies that norgalanthamine prevents nuclear translocation of Nrf-2 and by extension

its downstream effects on CCl₄-injured liver, thereby protecting hepatocytes against oxidative stress.

Acute experimental liver injury induced by CCl₄ drastically decreases the activities of the main liver P450 isoenzymes such as CYP1A2 and CYP2E1, as well as their protein expression (Song *et al.*, 2011; Xie *et al.*, 2014). The results of this study show that CYP1A2 mRNA expression increased in the norgalanthamine-treated groups. It is thought that norgalanthamine inhibits CYP1A2, which is involved in CCl₄ metabolism in the liver.

This study further examined the effects of norgalanthamine on lipid metabolism, which is an important pathological event, and on protective and/or therapeutic targets in liver disease (Musso *et al.*, 2017; Seo *et al.*, 2015). In the treatment of patients with nonalcoholic steatohepatitis, a molecular target of therapy is the PPAR-mediated increase in the oxidation of free fatty acids (Musso *et al.*, 2017). PPAR- γ participates in the modulation of metabolic disorders by activating the expression of genes involved in adipocyte maturation, lipid accumulation, and insulin-sensitive glucose transport (Lee *et al.*, 2017; Nagai *et al.*, 2009). These findings imply the potential of norgalanthamine as an anti-adipogenic agent, based on its ability to reduce lipid accumulation in the livers of mice with CCl₄-induced liver injury.

Among the notable features of CCl₄-induced liver injury are macrophage/Kupffer cell activation (Ahn *et al.*, 2016) and the induction of several genes that encode cytokines, including TNF- α , IL-1 β , and MCP-1, one of the key chemokines regulating the migration and infiltration of monocytes/macrophages (Deshmane *et al.*, 2009). These results show that norgalanthamine treatment suppressed both macrophage infiltration and the levels of all three cytokines in the

mouse liver. Thus, the hepatoprotective role of norgalanthamine seems to be associated with its anti-inflammatory effects and decreased activation of macrophages/Kupffer cells.

In chronic liver disease, as well as in the CCl₄-induced chronic-liver-injury animal model, hepatic fibrosis is accompanied by excessive accumulation of extracellular matrix proteins including α -SMA and fibronectin (Bataller and Brenner, 2005; Brancaccio *et al.*, 2018; Liu *et al.*, 2016). In this study, we found that the presence of collagen fibers (positive areas of PSR staining) and hydroxyproline, and expression of α -SMA and fibronectin were significantly increased in the CCl₄-induced chronic-liver-injury model. Of note, collagen fibers and hydroxyproline levels were significantly reduced in the norgalanthamine-treated group compared to the vehicle-treated control group, but no significant difference was observed between the silymarin-treated and vehicle-control groups. This implies that norgalanthamine administration is a candidate as an effective treatment option to reduce fibrosis in chronic liver disease through inhibition of α -SMA and fibronectin expression.

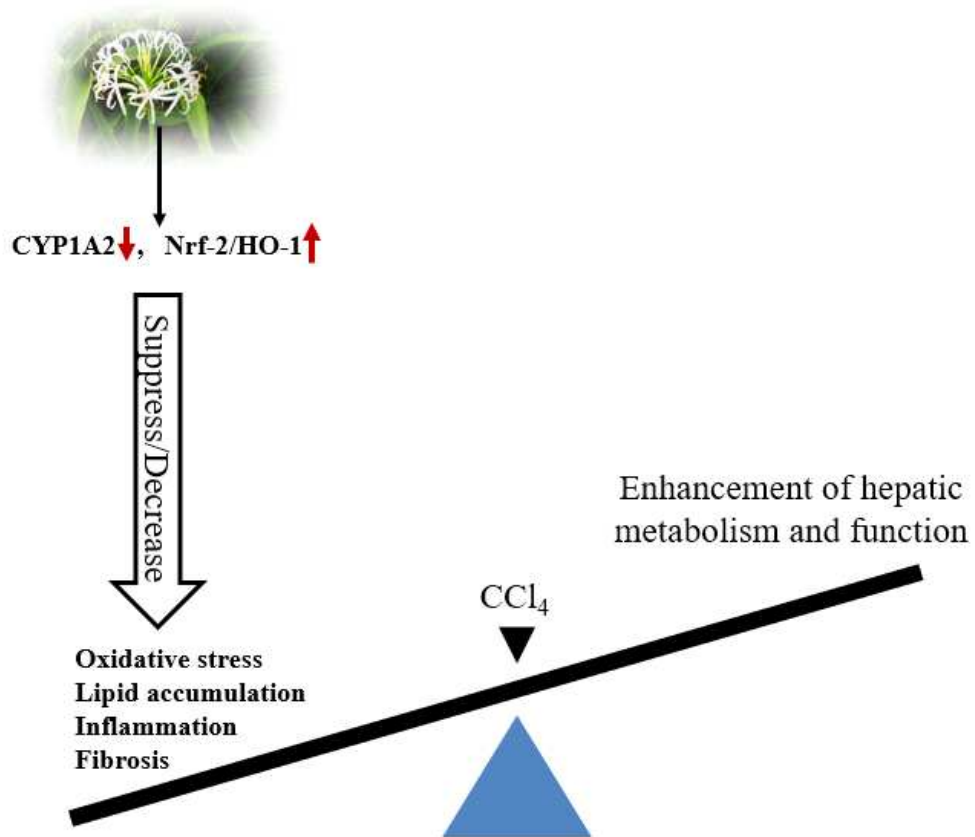


Figure 15. Schematic diagram of the proposed molecular effects of norgalanthamine in mice with CCl₄-induced liver injury.

In conclusion, in our mouse model of liver injury, norgalanthamine suppressed oxidative stress, hepatic lipid accumulation, and inflammation via activation of antioxidant molecules and down-regulation of adipogenic markers associated with lipid accumulation, pro-inflammatory mediators and anti-fibrosis factors. Overall, the hepatoprotective effects of norgalanthamine in the CCl₄ mouse model imply its therapeutic utility for treating liver injury (Fig. 15).

References

- Ahn, M., Park, J.S., Chae, S., Kim, S., Moon, C., Hyun, J.W., Shin, T., 2014. Hepatoprotective effects of *Lycium chinense* Miller fruit and its constituent betaine in CCl₄-induced hepatic damage in rats. *Acta Histochem* 116(2), 1104-1112.
- Ahn, M., Kim, J., Bang, H., Moon, J., Kim, G.O., Shin, T., 2016. Hepatoprotective effects of allyl isothiocyanate against carbon tetrachloride-induced hepatotoxicity in rat. *Chem Biol Interact* 254, 102-108.
- Badger, D.A., Sauer, J.M, Hoglen, N.C., Jolley, C.S., Sipes, I.G., 1996. The role of inflammatory cells and cytochrome P450 in the potentiation of CCl₄-induced liver injury by a single dose of retinol. *Toxicol Appl Pharmacol* 141(2), 507-519.
- Bansal, M.B., Kovalovich, K., Gupta, R., Li, W., Agarwal, A., Radbill, B., Alvarez, C.E., Safadi, R., Fiel, M.I., Friedman, S.L., Raub, R.A., 2005. Interleukin-6 protects hepatocytes from CCl₄-mediated necrosis and apoptosis in mice by reducing MMP-2 expression. *J Hepatol* 42(4), 548-556.
- Bataller, R., Brenner, D.A., 2005. Liver fibrosis. *J Clin Invest* 115(2), 209-218.
- Brancaccio, M., D'Argenio, G., Lembo, V., Palumbo, A., Catellano, I., 2018. Antifibrotic effect of marine ovothiol in an *in vivo* model of liver fibrosis. *Oxid Med Cell Longev* 2018, 5045734, 1-10.

- Cao, M., Wang, H., Guo, L., Yang, S., Liu, C., Khor, T.O., Yu, S., Kong, A.N., 2017. Dibenzoylmethane Protects Against CCl₄-Induced Acute Liver Injury by Activating Nrf2 via JNK, AMPK, and Calcium Signaling. *AAPS J* 19(6), 1703-1714.
- Dai, C., Xiao, X., Li, D., Tun, S., Wang, Y., Velkov, T., Tang, S., 2018. Chloroquine ameliorates carbon tetrachloride-induced acute liver injury in mice via the concomitant inhibition of inflammation and induction of apoptosis. *Cell Death Dis* 9, 1164.
- Decker, K., 1990. Biologically active products of stimulated liver macrophages (Kupffer cells). *Eur J Biochem* 192(2), 245-261.
- Deshmane, S.L., Kremlev, S., Amini, S., Sawaya, B.E., 2009. Monocyte chemoattractant protein-1 (MCP-1): an overview. *J Interferon Cytokine Res* 29(6), 313-326.
- Gavish, L., Perez, L.S., Reissman, P., Gertz, S.D., 2008. Irradiation with 780 nm diode laser attenuates inflammatory cytokines but upregulates nitric oxide in lipopolysaccharide-stimulated macrophages: implications for the prevention of aneurysm progression. *Lasers Surg Med* 40(5), 371-378.
- Hansen, H.H., Feigh, M., Veidal, S.S., Rigbolt, K.T., Vrang, N., Fosgerau, K., 2017. Mouse models of nonalcoholic steatohepatitis in preclinical drug development. *Drug Discov Today* 22(11), 1707-1718.

- Jiang, W., Li, M., He, F., Bian, Z., He, Q., Wang, X., Yao, W., Zhu, L., 2016. Neuroprotective effect of asiatic acid against spinal cord injury in rats. *Life Sci* 157, 45-51.
- Kang, J.I., Choi, J.H., Lee, J.G., Yoo, E.S., Kim, Y.H., Kang, H.K., 2017. The Mechanism of *Crinum asiaticum* var. *japonicum* on the Activation of Anagen. *Kor J Pharmacogn* 48(2), 148-154.
- Kensler, T.W., Wakabayashi, N., Biswal, S., 2007. Cell survival responses to environmental stresses via the Keap1-Nrf2-ARE pathway. *Annu Rev Pharmacol Toxicol* 47, 89-116.
- Kim, H.Y., Kim, J.K., Choi, J.H., Jung, J.Y., Oh, W.Y., Kim, D.C., Lee, H.S., Kim, Y.S., Kang, S.S., Lee, S.H., Lee, S.M., 2010. Hepatoprotective effect of pinoresinol on carbon tetrachloride-induced hepatic damage in mice. *J Pharmacol Sci* 112(1), 105-112.
- Kim, Y., Kim, J., Ahn, M., Shin, T., 2017. Lithium ameliorates rat spinal cord injury by suppressing glycogen synthase kinase-3beta and activating heme oxygenase-1. *Anat Cell Biol* 50(3), 207-213.
- Lee, C.W., Seo, J.Y., Lee, J., Choi, J.W., Cho, S., Bae, J.Y., Sohng, J.K., Kim, S.O., Kim, J., Park, Y.I., 2017. 3-O-Glucosylation of quercetin enhances inhibitory effects on the adipocyte differentiation and lipogenesis. *Biomed Pharmacother* 95, 589-598.

- Li, S., Hong, M., Tan, H.Y., Wang, N., Feng, Y., 2016. Insights into the role and interdependence of oxidative stress and inflammation in liver diseases. *Oxid Med Cell Longev* 2016, 4234061, 1-21.
- Li, S.Q., Wang, D.M., Shu, Y.J., Wan, X.D., Xu, Z.S., Li, E.Z., 2013. Proper heat shock pretreatment reduces acute liver injury induced by carbon tetrachloride and accelerates liver repair in mice. *J Toxicol Pathol* 26(4), 365-373.
- Liu, W., Wang, Z., Hou, J.G., Zhou, Y.D., He, Y.F., Jiang, S., Wang, Y.P., Ren, S., Li, W., 2018a. The Liver Protection Effects of Maltol, a Flavoring Agent, on Carbon Tetrachloride-Induced Acute Liver Injury in Mice via Inhibiting Apoptosis and Inflammatory Response. *Molecules* 23(9), 2120.
- Liu, X.Y., Liu, R.X., Hou, F., Cui, L.J., Li, C.Y., Chi, C., Yi, E., Wen, Y., Yin, Ch.H., 2016. Fibronectin expression is critical for liver fibrogenesis in vivo and in vitro. *Mol Med Rep* 14(4), 3669-3675.
- Liu, Y., Wen, P.H., Zhang, X.X., Dai, Y., He, Q., 2018b. Breviscapine ameliorates CCl₄-induced liver injury in mice through inhibiting inflammatory apoptotic response and ROS generation. *Int J Mol Med* 42(2), 755-768.
- Ma, J.Q., Li, Z., Xie, W.R., Liu, C.M., Liu, S.S., 2015. Quercetin protects mouse liver against CCl₄-induced inflammation by the TLR2/4 and MAPK/NF- κ B pathway. *Int Immunopharmacol* 28(1), 531-539.
- McGill, M.R., Jaeschke, H., 2019. Animal models of drug-induced liver injury.

Biochim Biophys Acta Mol Basis Dis 1865(5), 1031-1039.

Munakarmi, S., Chand, L., Shin, H.B., Jang, K.Y., Jeong, Y.J., 2020. Indole-3-Carbinol Derivative DIM Mitigates Carbon Tetrachloride-Induced Acute Liver Injury in Mice by Inhibiting Inflammatory Response, Apoptosis and Regulating Oxidative Stress. *Int J Mol Sci* 21(6), 2048.

Musso, G., Cassader, M., De Michieli, F., Paschetta, E., Pinach, S., Saba, F., Bongiovanni, D., Framarin, L., Berrutti, M., Leone, N., Corvisieri, S., Parente, R., Molinaro, F., Sircana, A., Bo, S., Gambino, R., 2017. MERTK rs4374383 variant predicts incident nonalcoholic fatty liver disease and diabetes: role of mononuclear cell activation and adipokine response to dietary fat. *Hum Mol Genet* 26(9), 1747-1758.

Nagai, Y., Yonemitsu, S., Erion, D.M., Iwasaki, T., Stark, R., Weismann, D., Dong, J., Zhang, D., Jurczak, M.J., Loffler, M.G., Cresswell, J., Yu, X.X., Murray, S.F., Bhanot, S., Monia, B.P., Bogan, J.S., Samuel, V., Shulman, G.I., 2009. The role of peroxisome proliferator-activated receptor gamma coactivator-1 beta in the pathogenesis of fructose-induced insulin resistance. *Cell Metab* 9(3), 252-264.

Nelson, D.R., Zeldin, D.C., Hoffman, S.M., Maltais, L.J., Wain, H.M., Nebert, D.W., 2004. Comparison of cytochrome P450 (CYP) genes from the mouse and human genomes, including nomenclature recommendations for genes, pseudogenes and alternative-splice variants. *Pharmacogenetics* 14(1), 1-18.

Ni, X., Wang, H., 2016. Silymarin attenuated hepatic steatosis through regulation of

lipid metabolism and oxidative stress in a mouse model of nonalcoholic fatty liver disease (NAFLD). *Am J Transl Res* 8(2), 1073-1081.

Rahman, T.M., Hodgson, H.J., 2000. Animal models of acute hepatic failure. *Int J Exp Pathol* 81(2), 145-157.

Recknagel, R.O., Glende, E.A. Dolak, J.A., Waller, R.L., 1989. Mechanisms of carbon tetrachloride toxicity. *Pharmacol Ther* 43(1), 139-154.

Rocha, S.W.S., Franca, M.E.R., Rodrigues, G.B., Barbosa, K.P.S., Nunes, A.K.S., Pastor, A.F., Oliveira, A.G.V., Oliveira, W.H., Luna, R.L.A., Peixoto, C.A., 2014. Diethylcarbamazine reduces chronic inflammation and fibrosis in carbon tetrachloride-(CCl₄-) induced liver injury in mice. *Mediators Inflamm* 2014, 696383, 1-15.

Russmann, S., Kullak-Ublick, G.A., Grattagliano, I., 2009. Current concepts of mechanisms in drug-induced hepatotoxicity. *Curr Med Chem* 16(23), 3041-3053.

Scholten, D., Trebicka, J., Liedtke, C., Weiskirchen, R., 2015. The carbon tetrachloride model in mice. *Lab Anim* 49(1 Suppl), 4-11.

Seo, Y.S., Kang, O.H., Kim, S.B., Mun, S.H., Kang, D.H., Yang, D.W., Choi, J.G., Lee, Y.M., Kang, D.K., Lee, H.S., Kwon, D.Y., 2015. Quercetin prevents adipogenesis by regulation of transcriptional factors and lipases in OP9 cells. *Int J Mol Med* 35(6), 1779-1785.

- Singh, D., Cho, W.C., Upadhyay, G., 2016. Drug-Induced Liver Toxicity and Prevention by Herbal Antioxidants: An Overview. *Front Physiol* 6, 363.
- Son, G., Iimuro, Y., Seki, E., Hirano, T., Kaneda, Y., Fujimoto, J., 2007. Selective inactivation of NF- κ B in the liver using NF- κ B decoy suppresses CCl₄-induced liver injury and fibrosis. *Am J Physiol Gastrointest Liver Physiol* 293(3), G631-G639.
- Song, S.Z., Choi, Y.H., Jin, G.Y., Li, G.Z., Yan, G.H., 2011. Protective effect of cornuside against carbon tetrachloride-induced acute hepatic injury. *Biosci Biotechnol Biochem* 75(4), 656-661.
- Tipoe, G.L., Leung, T.M., Liong, E.C., Lau, T.Y., Fung, M.L., Nanji, A.A., 2010. Epigallocatechin-3-gallate (EGCG) reduces liver inflammation, oxidative stress and fibrosis in carbon tetrachloride (CCl₄)-induced liver injury in mice. *Toxicology* 273(1-3), 45-52.
- Truong, N.H., Nguyen, N.H., Le, T.V., Vu, N.B., Huynh, N., Nguyen, T.V., Le, H.M., Phan, N.K., Pham, P.V., 2016. Comparison of the Treatment Efficiency of Bone Marrow-Derived Mesenchymal Stem Cell Transplantation via Tail and Portal Veins in CCl₄-Induced Mouse Liver Fibrosis. *Stem Cells Int* 2016, 5720413, 1-14.
- Unsal, V., Cicek, M., Sabancilar, İ., 2020. Toxicity of carbon tetrachloride, free radicals and role of antioxidants. *Rev Environ Health* 32970608.

- Vargas-Mendoza, N., Madrigal-Santillan, E., Morales-Gonzalez, A., Esquivel-Soto, J., Esquivel-Chirino, C., Garcia-Luna, Y., Gonzalez-Rubio M., Gayosso-de-Lucio, J.A., Morales-Gonzalez, J.A., 2014. Hepatoprotective effect of silymarin. *World J Hepatol* 6(3), 144-149.
- Wu, T., Zhang, Q., Song, H., 2018. Swertiamarin attenuates carbon tetrachloride (CCl₄)-induced liver injury and inflammation in rats by regulating the TLR4 signaling pathway. *Braz J Pharm Sci* 54(4), e177449.
- Xie, Y., Hao, H., Wang, H., Guo, C., Kang, A., Wang, G., 2014. Reversing effects of lignans on CCl₄-induced hepatic CYP450 down regulation by attenuating oxidative stress. *J Ethnopharmacol* 155(1), 213-221.
- Yang, B.Y., Zhang, X.Y., Guan, S.W., Hua, Z.C., 2015. Protective Effect of Procyanidin B2 against CCl₄-Induced Acute Liver Injury in Mice. *Molecules* 20(7), 12250-12265.
- Yoon, H.S., Kang, J.I., Kim, S.M., Ko, A., Koh, Y.S., Hyun, J.W., Yoon, S.P., Ahn, M.J., Kim, Y.H., Kang, J.H., Yoo, E.S., Kang, H.K., 2019. Norgalanthamine stimulates proliferation of dermal papilla cells via anagen-activating signaling pathways. *Biol Pharm Bull* 42(1), 139-143.
- Zeashan, H., Amresh, G., Singh, S., Rao, C.V., 2008. Hepatoprotective activity of *Amaranthus spinosus* in experimental animals. *Food Chem Toxicol* 46(11), 3417-3421.

Zou, J., Qi, F., Ye, L., Yao, S., 2016. Protective Role of Grape Seed Proanthocyanidins Against CCl₄ Induced Acute Liver Injury in Mice. Med Sci Monit 22, 880-889.

사염화탄소유도 간 손상 마우스 모델에서 노르갈란타민의 간 보호 효과 및 그 기전에 대한 연구

노르갈란타민(Norgalanthamine)은 제주도에서 자생하는 문주란 추출물의 주요 성분 중 하나이며, 털주머니의 증식을 통한 발모 촉진에 효과가 있다고 보고되었다. 이에 본 연구는 노르갈란타민이 사염화탄소로 유도되는 간 손상으로부터 간 보호 효과가 있음을 평가하기 위해 혈액생화학적 및 조직학적 검사를 실시하였고, 분자생물학적 기법을 이용하여 그 기전을 확인하였다.

사염화탄소유도 급성 간 손상 모델에서의 효능 평가는 노르갈란타민을 1 및 10 mg/kg 용량으로 1일 1회, 7일간 경구 투여한 후, corn oil과 동량 희석한 사염화탄소를 1.5ml/kg 용량으로 단회 복강투여하였다. 이후 만성 간 손상 모델에서의 효능 평가를 위해서 2주간 노르갈란타민을 투여하면서 3일마다 사염화탄소를 같은 용량으로 복강투여하였다. 정상 동물 대조군 및 사염화탄소 유도 대조군에는 동량의 PBS를 투여하였고, 간 보호 효과가 있는 것으로 알려진 silymarin 100 mg/kg 용량을 양성대조군으로 사용하였다.

혈액생화학적 검사 결과, 간 손상 지표 중 aspartate aminotransferase(AST), alanine aminotransferase (ALT) 및 총 빌리루빈(T-bil) 농도는 정상 동물군에 비해 대조군에서 유의성 있게 증가한 반면 노르갈란타민 투여군에서 유의성 있게 감소하였다.

조직학적 검사 결과, 노르갈란타민 투여에 의해 간의 중심 정맥 주위 괴사, 지방구의 침윤 정도 및 간조직의 섬유화가 대조군에 비해 유의성 있게 감소되었으며 cytochrome P4501A2 (CYP1A2)를 비교한 결과, 사염화탄소유도에 의해 감소되었고, 노르갈란타민 투여에 의해 유의성 있게 증가되었다. 또한 노르갈란타민에

의한 항산화 효과를 평가한 결과, 항산화효소인 superoxide dismutase 및 catalase가 대조군에 비해 유의성 있게 증가되었으며 간의 염증반응을 비교한 결과, tumor necrosis factor alpha와 interleukin 싸이토카인의 발현이 노르갈란타민 투여에 의해 유의적으로 감소되었고, monocyte chemoattractant protein-1 케모카인의 발현도 유사한 결과를 보였다. 다음으로 조직 내 ionized calcium binding adapter molecule-1 면역조직화학 염색을 통해 Kupffer cell 및 monocyte의 활성화 정도를 평가한 결과, 노르갈란타민 투여에 의해 그 발현이 유의성 있게 감소하였다. 지방생성 관련 유전자인 peroxisome proliferator-activated receptor gamma와 adipocyte protein-2의 발현도 노르갈란타민 투여에 의해 유의적으로 감소되는 것을 확인하였다. 간 섬유화와 관련된 α -SMA와 fibronectin의 발현도 노르갈란타민 투여에 의해 감소되었다. 또한 항산화 관련 인자인 nuclear factor erythroid 2-related factor 2 (Nrf-2) 및 heme oxygenase-1 (HO-1)의 발현을 확인한 결과, 노르갈란타민 투여로 간세포의 세포질에서 핵으로 Nrf-2가 전이된 발현이 증가되었고, 이로 인해 HO-1의 발현도 증가한 것을 확인하였다.

결론적으로 노르갈란타민은 사염화탄소유도 간 손상 모델에서 CYP1A2의 활성을 감소시키고, Nrf-2 및 HO-1의 활성화로 산화적 손상, 지방구 침윤, 염증 반응 및 섬유화를 완화시킴으로써 간을 보호한 것으로 판단된다.

주요어 : 간손상, 노르갈란타민(norgalanthamine), 사염화탄소(CCl₄), HO-1, Nrf-2

감사의 글

2007년 박사수료와 함께 유한양행에 입사해서 오늘까지 오랜 시간동안 졸업과 학위취득이라는 마침표를 찍지 못하고 침표상태로 지내오다 좋은 기회와 인연을 만나서 이런 감사의 글을 쓸 수 있는 기회를 얻게되어 누구보다 감회가 새롭습니다.

우선 갈 곳 없는 저를 흔쾌히 받아주셔서 뜻깊은 오늘이 있게 해주신 신태균 교수님께 가장 큰 감사를 드립니다.

또한, 존경하는 후배이자 멘토인 안미정 교수님이 상지대로 온 게 저에게는 너무나도 큰 행운이 되었습니다. 그로인해 좋은 기회를 얻을 수 있었고, 멀긴하지만 제 주보다는 가까운 원주를 오가면서 같이 실험한 덕분에 졸업이라는 값진 열매를 얻을 수 있었습니다. 오랫동안 갈망해왔지만 혼자서는 감히 이를 수 없었던 아픔을 알고 챙겨준 안교수님께 깊은 감사를 드립니다.

고명순 박사님, 바쁜 와중에도 부검과 샘플링, 그리고 많은 분석을 거리낌없이 발 벗고 도와주신 덕분에 좋은 결과를 얻을 수 있었습니다. 너무 고마워하지 않아도 된다는 그 말이 더욱 힘이 되었고 감사했습니다. 박사님처럼 저도 누군가에게 꼭 베풀도록하겠습니다.

심사위원 위촉에 흔쾌히 승낙해 주신 김승준 교수님, 문창종 교수님, 김희철 박사님께 너무나도 감사드립니다. 학창시절에 만났던 존경하는 선배님, 후배님을 이런 좋은 인연으로 세월이 흘러 다시 만날 수 있어서 너무나도 좋았고, 공개발표할때도 강당 정중앙 심사위원석에 신교수님 사단이 앉아 계셔서 떨지않고 당당하게 할 수 있었던 것 같습니다. 이제 그 든든한 울타리안에 들어갈 수 있게된 것 같아서 괜스레 뿌듯하고 내편이 생긴 듯해서 너무 좋습니다.

유한양행 김승현 과장님, 지경아 선생님께도 깊은 감사를 드립니다. 개인적인 실험을 부탁드렸음에도 기쁘게 도와주신 덕분에 좋은 결과를 실을 수 있게 되었습니다.

업무와 논문발표일정이 겹쳐서 시간에 쫓겨 눈물나게 힘든 시간을 두 분께서 도와 주시고 응원해주신 덕분에 무사히 잘 넘길 수 있었습니다. 항상 감사드립니다.

웨스턴 결과 분석을 위해서 밤낮으로 애써주시고, 공개발표 첫 번째 청중이 되어 주신 전지윤 후배님께도 깊은 감사를 드립니다.

부족하나마 병리라는 분야를 계속할 수 있도록 이끌어 주셨던 배종희 교수님, 오랜만에 찾아간 학교에서 반갑게 맞아주시고 직접 공개발표장에 오셔서 발표자료를 꼼꼼하게 챙겨주신 정종태 교수님께도 감사드립니다.

논문발표 준비하느라 바쁜 와중에 갑상선암 수술을 받느라 딸 간호도 제대로 못 받으시면서도 저를 먼저 챙겨주신 사랑하는 어머니, 이 세상 누구보다 든든한 버팀목이 되는 사랑하는 동생 홍일 & 정미, 마지막으로 세상 무엇과도 바꿀 수 없이 가장 사랑하는 귀요미 조카 은후. 사랑하는 가족이 있어서 곳곳이 버틸 수 있는 힘을 얻을 수 있고 부끄럽지 않은 사람이 되기 위해서 항상 열심히 살겠습니다. 우리 가족이 힘든 시기에 조금이나마 귀한 선물을 드릴 수 있게 되어서 감사하게 생각합니다.

대학교 졸업이후부터 지금까지 시간을 돌이켜봤을 때 故 이국경 교수님 덕분에 유한양행 연구소까지 올 수 있지 않았나 싶습니다. 이런 좋은 날을 맞은 것도 교수님께서 하늘에서 지켜봐 주시고 응원해주신 덕분이라 생각합니다. 잊지 않겠습니다.

2020년 하반기는 1분 1초에 쫓기면서 정신없이 그 어느때보다 바쁘게 보낸 시간이었습니다. 하지만 그 시간들속에서 좋은 인연을 만날 수 있었고 수 없이 많은 감사함을 느꼈던 시간이었습니다. 이 지면에 다 적지는 못했지만 항상 옆에서 응원해주시는 고마운 분들, 더러는 서러움과 시련을 주기도 하지만 거기서 또 새로운 힘을 얻을 수 있는 강인함을 가르쳐 주신 분들 덕분에 삶을 살아갈 수 있는 것 같습니다. 모든 분들께 감사드립니다.